several heterologous proteins conferred such an effect. We suggest that the resulting modified Gag-based lentiviral vector can serve as a next generation lentiviral vector system, and should contribute to diverse applications of the lentiviral vector.

Results

We constructed HIV-1 Gag constructs (Figure 1a) containing the following PM-targeting proteins or PM-targeting signals fused to the Gag amino-terminus: the transmembrane proteins CD4, CD8, CXCR4, HIV-1 *Env*, or the acylation signal motifs of *lyn*, Gα(12), Gα(13) and Gα(16). This makes the original Gag myr signal unable to function. For CD4 and CXCR4, the full-length (FL) and cytoplasmic tail-deleted derivatives (DC) were examined. The membrane protein mutants are expected to traffic to the PM through the vesicular trafficking pathway involving ER and Golgi apparatus. As *lyn* encodes two overlapping acylation motifs, a myr and palmitoylation (pal) motif, we generated three *lyn*-derived constructs bearing a myr signal only, a pal signal only, or both signals (denoted myr^{lyn}, pal^{lyn}, myr/pal^{lyn}). In the *lyn* myr signal constructs, the position of the myristoyl group is –22 amino acids upstream from the original Gag context (denoted wild type, WT, hereafter). The *gag* and *env* sequences were human codon-optimized. The start codon and myr signal of Gag were destroyed by the M1L and G2A mutations to avoid internal translational initiation that could influence the experimental results.[14] The myr signal-defective Gag construct G2A was used as a negative control. PH-*gag* was used as a positive control that showed enhanced viral production.[14] The Gα(12), Gα(13) and Gα(16) constructs have one, two and three pal attachment sites, respectively. All the constructs were fused to green fluorescent protein (GFP), and expression was verified by western blot and immunoprecipitation analyses (Figure 1b).

A confocal microscopic analysis revealed that the majority of Gag-GFP was targeted to the PM, but some Gag-GFP was distributed in the cytoplasm with a fine vesicular pattern in 293T cells (Figure 1c, WT). G2A-GFP showed a homogenous cytoplasmic distribution (Figure 1c). PH-Gag-GFP showed a distribution pattern similar to the WT (Figure 1c). These data are consistent with our previous findings.[14] The membrane protein Gag constructs mostly accumulated in the perinuclear region and only some of the protein was targeted to the PM, as verified by flow cytometric analysis using antibodies recognizing the extracellular domain of CD4, CD8 or CXCR4 (exemplified by the CXCR4^{FL} mutant in Figure 1c, and data not shown). The myr/pal^{lyn} construct showed a phenotype similar to WT with fine vesicular staining close to the nucleus (Figure 1c). The myr^{lyn} construct showed a PM-targeting phenotype similar to WT (Figure 1c). The pal^{lyn} construct was distributed evenly in the cytoplasm similar to G2A (Figure 1c). The Gα constructs were distributed predominantly in the cytoplasm with vesicular staining patterns, and less evidently at the PM (exemplified by the Gα(16) construct in Figure 1c).

To evaluate the efficiency of virus-like particle (VLP) production, we measured the GFP fluorescence intensity of culture supernatants containing VLP relative to the cell fraction (Figure 1d). PH-*gag* showed a significant enhancement of VLP production (229.0%, Figure 1d) compared with Gag-GFP, and the G2A construct produced almost no VLP, consistent with previous findings.[14] Membrane protein mutants produced little VLP (0.8–41.6% relative to Gag-GFP), presumably because they were inefficiently transported to the PM as evidenced by the confocal microscopy analysis (Figure 1c). Among the membrane protein mutants, CXCR4^{FL}-*gag*-GFP showed the best VLP production efficiency (41.6% relative to Gag-GFP). Interestingly, deleting the cytoplasmic tail of CXCR4 led to a drastic loss of VLP production (0.8% relative to Gag-GFP), suggesting that the cytoplasmic tail of CXCR4 somehow contributes to VLP production. Myr/pal^{lyn}-*gag*-GFP showed significantly greater VLP production than the WT (229.4%, $P<0.05$, Student's *t*-test). Myr^{lyn}-*gag*-GFP produced slightly more VLP than the WT (131.5%). Pal^{lyn}-*gag*-GFP showed a weak VLP production ability (14.1%), possibly because the pal signal did not function effectively, or the palmitoyl group did not function as a PM-targeting motif in the given protein context. The Gα(12)- and Gα(13)-*gag*-GFP constructs, containing one or two pal motifs, respectively, showed 7.0 and 7.3% VLP production efficiencies, compared with the WT. The Gα(16)-*gag*-GFP construct, containing three pal motifs, was able to produce VLP (28.8%) more effectively than the other Gα constructs, suggesting that the pal group serves as a weak PM-targeting motif and that the motifs function additively. The two- to threefold enhancement of VLP production by PH- and myr/pal^{lyn}-gag-GFP was verified by western blot analysis examining the VLP fraction (data not shown). Overall, the GFP fluorescence-based VLP production assays were consistent with the microscopy observations indicating that the constructs that were able to target Gag to the PM were competent in VLP production (Figure 1c). These data indicate that the Gag constructs carrying *lyn* myr/pal or myr signals support VLP production more efficiently than the WT. Thus, we examined the infectivity of the lentiviral vectors produced by Gag with heterologous myr signals.

We constructed *gag-pol* derivatives bearing the myr/pal^{lyn} or myr^{lyn} sequences, and additional myr signal constructs carrying the myr signal of HIV-1 or MLV MA (myr^{HIV-1}- or myr^{MLV}-*gag-pol*, Figure 1a). These constructs were generated to examine whether any heterologous myr signal can function to enhance VLP production similar to the effect of the *lyn* acylation signal. In myr^{HIV-1}- or myr^{MLV}-*gag-pol*, the position of the myristoyl group is –22 amino acids upstream from the original Gag context, which is similar to the same position as myr/pal^{lyn} and myr^{lyn} mutants (Figure 1a). The expression of the *gag-pol* derivatives was verified by western blot analysis in which Pr55^{Gag} and its cleaved products by viral protease including MA-CA and p24^{CA} were detected (Figure 2a). These mutants produced VLP in the culture supernatant as verified by western blot analysis (Figure 2b). Using these *gag-pol* expression plasmids, in combination with the luciferase-encoding gene transfer plasmid and expression plasmids for Rev and VSV-G, we produced a lentiviral vector in 293T cells. The viral production efficiencies were assessed by measuring the amount of viral capsid antigen p24^{CA}

a

```
Gag                                                    MGARASVL...
G2A                                                    MAARASVL...
PH-gag                          (PLC delta 1 aa 1-175)-PRAE FTLAARASVL...
CD4FL-gag                                 (CD4 aa 1-458)-E FTLAARASVL...
CD4DC-gag                                 (CD4 aa 1-424)-E FTLAARASVL...
CXCR4FL-gag                     (CXCR4 aa 1-352)-EISSSSFE FTLAARASVL...
CXCR4DC-gag                      (CXCR4 aa 1-308)-ISSSSFE FTLAARASVL...
CD8-gag                 (CD8 aa 1-235)-IDLELKL RILQSSSSFE FTLAARASVL...
Env-gag                       (Env aa 1-869)-D PATGLRSRAE FTLAARASVL...
myr/palLyn-gag                      MGCIKSKRKD NLNDDERRAE FTLAARASVL...
myrLyn-gag                          MGAIKSKRKD NLNDDERRAE FTLAARASVL...
palLyn-gag                          MACIKSKRKD NLNDDERRAE FTLAARASVL...
Galpha(12)-gag                   MS GVVRTLSRCL LPAEAGRRAE FTLAARASVL...
Galpha(13)-gag                 MAD FLPSRSVCFP GCVLTNRRAE FTLAARASVL...
Galpha(16)-gag               MARSL RWRCCPWCLT EDEKAARRAE FTLAARASVL...
myrHIV-1-gag                        MGARASVLSG GELDRWRRAE FTLAARASVL...
myrMLV-gag                          MGQTVTTPLS LTLGHWRRAE FTLAARASVL...
```

b

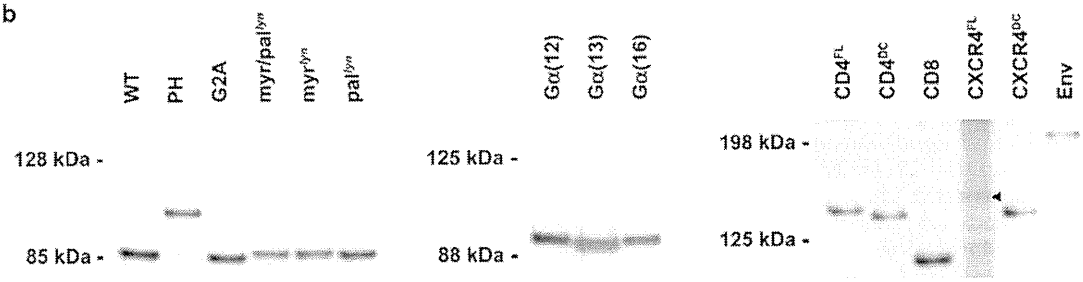

c

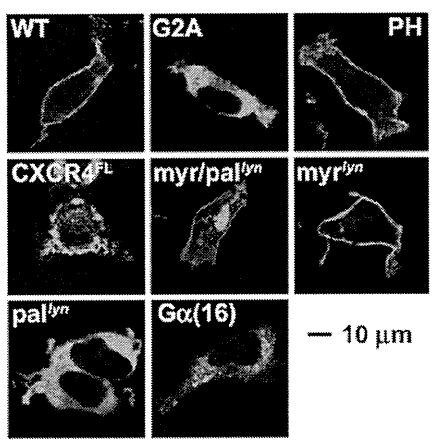

d VLP production efficiency (GFP fluorecence of VLP / cell fractions)

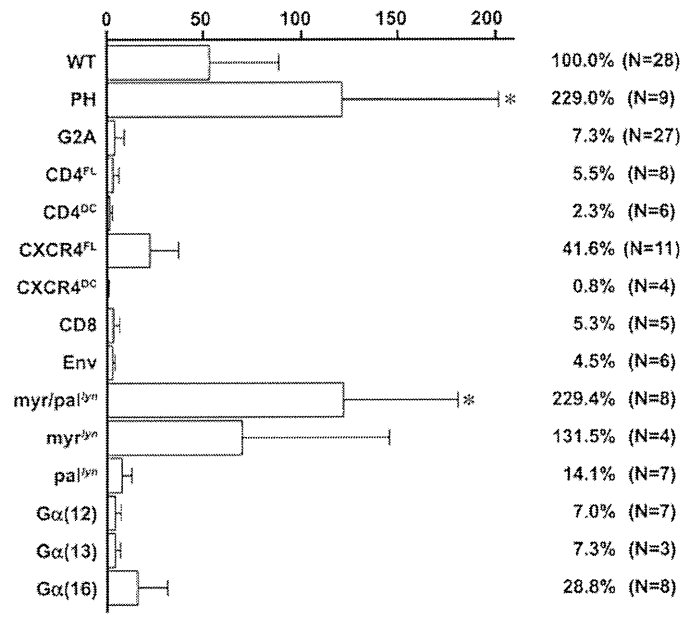

Figure 1 The production of VLPs by genetic modification of the PM-targeting signal of Gag. (**a**) The mutants used in this study. The myr site is marked with a dot, the palmitoylation site with an underline. The Gag translational initiation site and the myr target residues were mutated to leucine and alanine to minimize internal translational initiation and myr. (**b**) The verification of protein expression of Gag-GFP derivatives in 293T cells by western blot analysis using anti-FLAG antibody. All the constructs carry the FLAG epitope at the C-terminus of Gag. The CXCR4^{FL}-Gag-GFP showed a low efficiency of detection, thus the immunoprecipitation was performed before immunoblotting (triangle). (**c**) The distribution of Gag-GFP derivatives in 293T cells examined by confocal microscopy. WT represents the Gag-GFP, and the membrane-targeting signals are shown at the top of each panel. The bar represents 10 μm, magnification ×630. (**d**) VLP production efficiency of Gag-GFP derivatives measured by the GFP fluorescence in the VLP fraction divided by that of the cell fraction. The average and s.d. of the indicated number of independent experiments are shown. The VLP production efficiency relative to Gag-GFP is shown as a percentage at the right. Asterisks indicate the statistical significance compared with Gag-GFP by two-tailed Student's *t*-test ($P<0.05$).

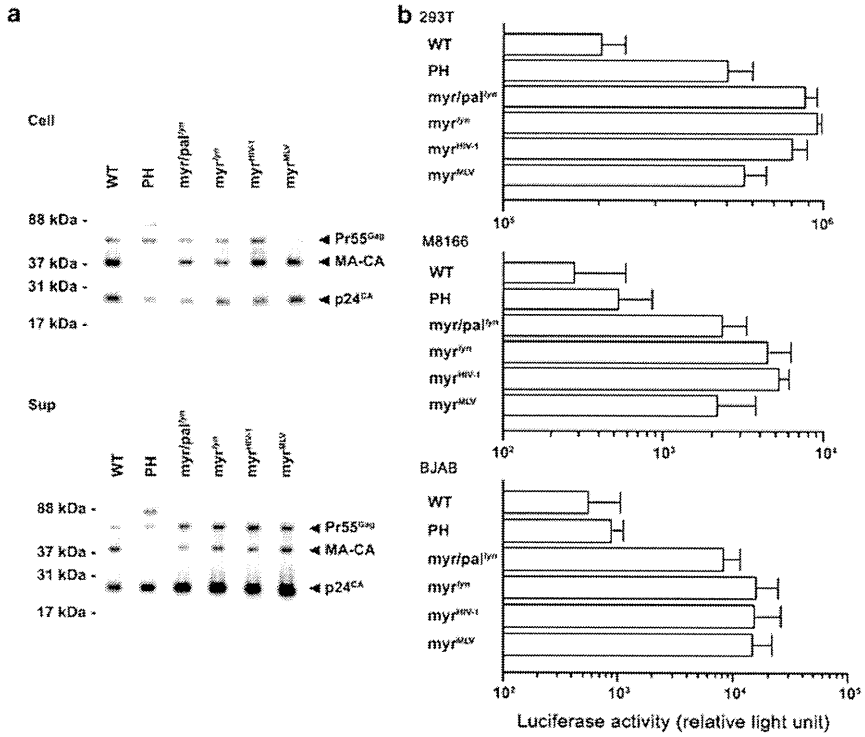

Figure 2 Lentiviral vector production and infectivity of myr signal mutants. (**a**) Verification of protein expression and VLP production of *gag-pol* derivatives in 293T cells by western blot analysis using anti-p24^{CA} antibody. The upper panel shows the analysis of cell lysate equivalent to $1 \sim 2 \times 10^5$ cells (Cell). The lower panel shows the viral particles collected from the culture supernatant (Sup). Pr55^{Gag} ($\sim$55 kDa), the proteolytic cleavage intermediate of Pr55^{Gag} (MA-CA, $\sim$40 kDa) and the complete proteolytic cleavage product p24^{CA} ($\sim$24 kDa) are indicated by arrowheads. PH-Gag has a higher molecular weight precursor and intermediate because of the PH domain of 23 kDa attached to the MA domain. (**b**) The transduction efficiency of the luciferase gene into various cell types. The 293T, M8166 and BJAB cells were tested for luciferase gene transduction by the myr signal derivative lentivirus vectors. The *x* axis represents relative light emission. The average ± s.d. of luciferase activity assay in quadricate (293T) or in triplicate (M8166 and BJAB) was shown. A representative data from three independent experiments is shown.

in the culture supernatant by enzyme-linked immunosorbent assay (ELISA). Enhancement of virus production by the PH, myr/pal^{lyn} and myr^{lyn} constructs was observed (4.1-, 6.3- and 10.5-fold increase in production, respectively, relative to the WT, Table 1). These data are consistent with the western blot analysis in which the levels of p24^{CA} are decreased from the cell fraction and increased in the VLP fraction for PH and myr signal mutants (Figure 2a). The magnitude of viral production enhancement was augmented in the *gag-pol* context compared with the Gag-GFP context. This is explained by the efficiency of Gag cleavage in the virion as described below. Viral production by the myr^{HIV-1}- or myr^{MLV}-*gag-pol* constructs also increased (6.2- or 6.1-fold, respectively, Table 1), suggesting that any heterologous myr signal can increase the production of lentiviral vector.

Luciferase gene transduction by lentiviral vectors produced using the modified Gag-pol was assessed in 293T cells. The gene transduction efficiencies of *gag-pol* constructs were 6.1- to 10.9-fold greater than the WT (Figure 2b and Table 1). The luciferase activity decreased on treatment of the cells with the reverse transcriptase inhibitor nevirapine, suggesting that the luciferase activity indeed represents lentiviral gene transduction (data not shown). The increase in viral production by the heterologous myr signal constructs (4.3- to 7.8-fold compared with WT) largely agrees with the level of augmentation of luciferase activity (5.7- to 10.4-fold, Table 1). The myr/pal^{lyn} mutant showed a higher ratio (1.7) of luciferase transduction efficiency relative to viral production than the other myr signal mutants,

Table 1 Summary of viral production and infectivity of myr signal Gag mutants

	Viral production[a]	*Luciferase transduction*[b]	*Ratio*[c]
WT	1.0 ± 0.0 ($n = 17$)	1.0 ± 0.0 ($n = 15$)	1.0
PH	4.1 ± 0.9 ($n = 17$)**	6.3 ± 1.8 ($n = 15$)*	1.5
myr/pal^{lyn}	6.3 ± 1.8 ($n = 17$)*	10.4 ± 2.7 ($n = 15$)**	1.7
myr^{lyn}	10.5 ± 3.4 ($n = 13$)*	9.2 ± 3.2 ($n = 11$)*	0.9
myr^{HIV-1}	6.2 ± 1.9 ($n = 12$)*	5.7 ± 1.5 ($n = 10$)*	0.9
myr^{MLV}	6.1 ± 1.1 ($n = 12$)**	7.6 ± 2.7 ($n = 10$)*	1.2

Abbreviations: HIV-1, human immunodeficiency virus type 1; MLV, murine leukemia virus; myr, myristoylation; pal, palmitoylation; PH, pleckstrin homology; WT, wild type.
[a]The average ± s.e.m. of the p24^{CA} concentration relative to WT from the indicated number of independent experiments.
[b]The average ± s.e.m. of transduced luciferase activity relative to WT from the indicated number of independent experiments.
[c]The luciferase transduction divided by viral production.
Asterisks indicate a statistically significant difference compared to the WT by two-tailed Student's paired *t*-test (*$P < 0.05$, **$P < 0.01$).

suggesting that the infectivity of the myr/pal^{lyn} virus particles is slightly improved (Table 1). Luciferase gene transduction by myr signal constructs was also observed in the B lymphoid cell line BJAB and T lymphoid cell line M8166, similar to 293T cells (Figure 2b). Gene transduction of GFP by myr signal *gag-pol* constructs was comparable to transduction of the luciferase gene (data not shown). Collectively, these results indicate that extending the amino-terminus of Gag with a heterologous myr signal enhances infectious lentiviral production.

We analyzed the molecular mechanisms by which viral production was improved by the amino-terminal Gag modifications. We examined (i) the oligomerization efficiency, (ii) the Vps4-dependence of viral budding, (iii) Gag targeting to the Triton X-100-insoluble lipid (detergent-resistant membrane, DRM) fraction and (iv) the morphology of the virion. First, the oligomerization efficiency was measured using a bioluminescent resonance energy transfer (BRET) assay (Figure 3a). The 293T cells were co-transfected with plasmids expressing Gag derivatives fused to GFP or renilla luciferase (Rluc), and the GFP fluorescence activated by the Rluc-emitted light was measured in living cells. This BRET signal should represent the self-oligomerization efficiency of Gag derivatives *in vivo*. The GFP–Rluc fusion protein should yield the best BRET efficiency, and was thus used as the positive control. Rluc alone should not yield any BRET signal, and thus was used as a negative control. We focused on the derivatives that showed enhanced viral production. The BRET levels of all the tested mutants were significantly increased compared with the WT Gag (Figure 3a). These data imply that the assembly of the myr signal Gag constructs is more efficient than the WT. It is conceivable that the enhanced VLP production of myr signal Gag constructs is, in part, because of improved assembly efficiency. Efficient Gag assembly should also assist the Gag-pol assembly. The Gag-pol assembly leads to the activation of a viral protease that cleaves Gag to make the virus infectious. Provided that the myr signal Gag mutants can efficiently activate the viral protease, we expected that the Gag processing of myr signal Gag constructs should be more efficient than the WT. Virions were collected by centrifugation and processed for western blotting using the anti-p24^{CA} monoclonal antibody (mAb). Anti-p24^{CA} mAb binds to Pr55^{Gag} and its cleaved products including MA-CA and p24^{CA}. The p24^{CA} signal relative to the Pr55^{Gag} and MA-CA represents the Gag processing efficacy. Compared with cell lysates (Figure 2a), viral lysates showed better Gag cleavage for all samples (Figure 3b). The WT virions showed a substantial amount of Gag intermediates (Figure 3b). In contrast, only trace amounts of intermediate were detected in the myr signal construct virions (Figure 3b). It is possible that the enhanced Gag processing is due to the increased Gag-pol to Gag ratio in the virion produced by myr Gag mutants. We tested this possibility by western blot analysis probing p24^{CA} and integrase (IN) at the same time. IN represents the Gag-pol because IN is one of the proteolytic products generated from Gag-pol. The signal intensities of IN (open arrowhead, Figure 3b) relative to p24^{CA} (filled arrowhead, Figure 3b) for myr signal mutants were comparable to WT, suggesting that enhanced Gag processing is not due to the increased Gag-pol to Gag ratio in the virion

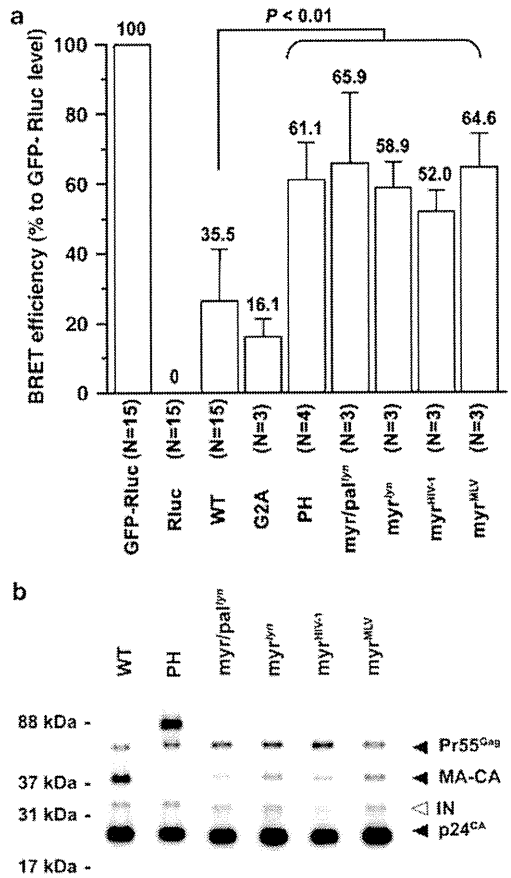

Figure 3 The physical and functional properties of myr signal derivatives of Gag. (**a**) Gag oligomerization examined by BRET analysis. The GFP–Rluc fusion protein and Rluc alone were used as positive and negative controls. The average ± s.d. of BRET efficiencies relative to the controls obtained in the indicated number of experiments are shown. All the *gag* mutants yielded significantly higher BRET signals than that of WT as analyzed by two-tailed Student's *t*-test ($P<0.01$). (**b**) The Gag processing and the Gag to Gag-pol ratio in the virion was tested by western blot analysis using anti-p24^{CA} and anti-IN monoclonal antibodies. Note that the samples were loaded to yield similar p24^{CA} signals to highlight the differences in Gag cleavage efficiencies and Gag to Gag-pol ratio. The virion was collected from the culture supernatant of cells shown in Figure 2a. Pr55^{Gag}, MA-CA, p24^{CA} (filled) and IN (open) are indicated by arrowheads.

produced by myr Gag constructs. Collectively, the results suggest that the heterologous myr signals enable Gag to assemble with a higher efficiency, leading to the activation of protease to process Gag more efficiently in the virion. This should account for the fact that the magnitude of difference between WT and mutants in VLP production was assessed greater by p24 ELISA assay using *gag-pol* constructs than by GFP fluorescence-based assay using Gag-GFP constructs.

Second, the Vps4-dependence of VLP budding was examined. Vps4 drives HIV-1 budding.[15] We measured VLP production efficiencies by *gag-pol* derivatives in the presence or absence of a dominant-negative Vps4. If VLP budding is powered by a Vsp4-independent mechanism, expression of dominant-negative Vps4 should not reduce the VLP production efficiency. Viral gene expression was

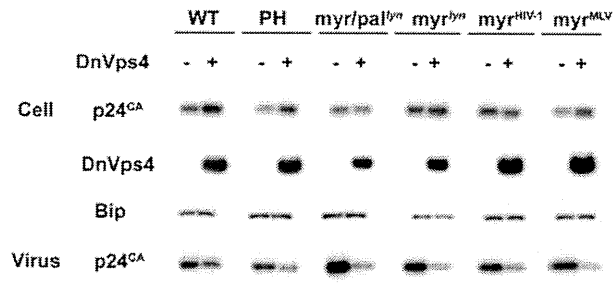

Figure 4 The effect of dominant-negative Vps4 (DnVps4) on virus production by acylation signal Gag derivatives. DnVps4 expression did not lower Gag expression in transiently transfected 293T cells. In contrast, the virus production by all the Gag constructs was inhibited by DnVps4, similar to the WT.

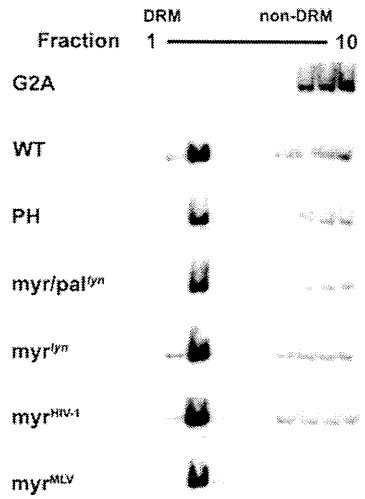

Figure 5 The targeting of Gag-GFP derivatives to the DRM fraction examined by a membrane floatation assay. G2A construct distributed to the non-DRM fractions (lanes 8–10), and WT Gag was targeted to the DRM (lanes 2–3). Other mutants distributed to the DRM fractions similar to WT Gag. All the derivatives were probed with anti-FLAG antibody.

not inhibited by dominant-negative Vps4 expression as judged by p24^{CA} levels (Figure 4). However, on expression of dominant-negative Vps4, viral production decreased in all the mutants (the lower panel of Figure 4), suggesting that the amino-terminal modification of Gag does not alter the molecular mechanism of viral budding.

Third, DRM targeting was examined using membrane floatation assays. Gag has previously been shown to form higher order complexes and bud at DRM-containing regions.[16,17] Increased viral production by myr signal Gag constructs may be due to improved efficiency of DRM targeting. In our experimental conditions, approximately 70% of Gag-GFP distributed to the DRM fractions (Figure 5). In contrast, G2A-GFP distributed predominantly to the non-DRM fractions (Figure 5). These data are consistent with the microscopy observations and previous reports (Figure 1c and Lindwasser and Resh[16] and Ono and Freed[17,18]). The myr signal derivatives accumulated in the DRM fractions at levels similar to the WT (Figure 5). These data suggest that enhanced viral production is not due to enhanced DRM targeting of Gag with amino-terminal modifications.

Finally, the morphology of the virion was analyzed using TEM. We compared the morphology of the WT and the myr^{lyn}-*gag-pol* virions. The morphology of budding and mature virions of myr^{lyn}-*gag-pol* construct was indistinguishable from the WT (Figure 6).[14] In addition, VSV-G was incorporated into the virion produced by myr signal derivatives at levels similar to the WT (data not shown). Similar observation was made for the incorporation of HIV-1 Env onto the virion (data not shown). The myr^{HIV-1}- and myr^{MLV}-Gag-GFP showed a PM-targeting phenotype similar to the WT as judged by confocal microscopy (data not shown). Taken together, lentiviral vectors bearing amino-terminally engineered Gag can produce virions with greater efficiencies than the original lentiviral vector. This increase was primarily attributed to the effects of the increased efficiency Gag oligomerization.

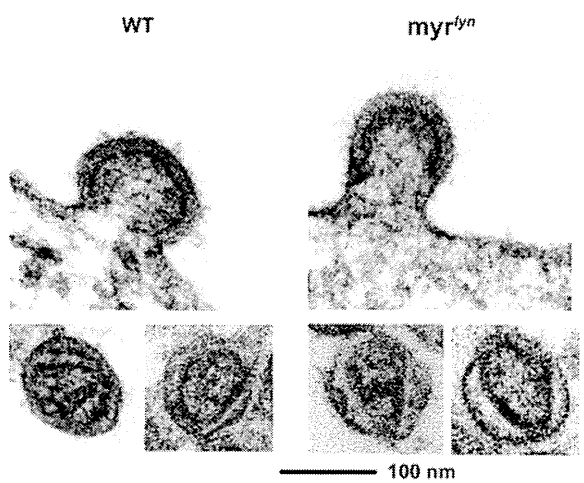

Figure 6 The morphology of virions produced from 293T cells transiently transfected with *gag-pol* (WT, left) or myr^{lyn}-*gag-pol* (right) expression vector. The upper panels show viral budding at the cell periphery, and the lower panels show the morphology of virions found in the extracellular space. The bar represents 100 nm, magnification × 50 000.

Discussion

In this study, we have provided evidence that genetic modification of the structural protein Gag can improve the virion production efficiency of the HIV-1-based lentiviral vector up to 10-fold. Our technology will provide an improved lentiviral vector for human gene therapy applications, which require large-scale viral vector preparation. Historically, efforts to improve the lentiviral vector have not involved the modification of the structural protein Gag.[9] Our strategy is unique in this regard. Our viral vector can be defined as a next generation lentiviral vector. This approach may also be worth testing for murine leukemia virus (MLV)-based vectors because the function of the MLV Gag is dependent on amino-terminal myr sites, similar to HIV Gag.

Our genetic approach revealed that amino-terminal modifications that re-position the myristoyl group attachment site on Gag can alter the late phases of the HIV-1 life cycle. Gag traffics to the PM efficiently, and the myristoyl group is critical for this process.[19] The myristoyl group attached to Gag is in equilibrium between exposed and folded 'hidden' conformations.[20] The PM targeting of Gag depends primarily on myristoyl group exposure. It is possible that re-positioning of the myristoyl group on Gag may slightly shift the structural equilibrium toward the exposed conformation, which facilitates PM targeting by Gag. However, myr signal Gag mutants did not show higher DRM-targeting efficiencies than WT (Figure 5). We performed the membrane floatation assay without Triton X-100 and found that the myr signal Gag mutants and WT distributed to the membrane fraction at similar efficiencies (data not shown). These data may suggest that the myristoyl group exposure model is unlikely. However, these data may not necessarily negate the myristoyl group exposure model because it is possible that the steady-state levels of Gag association with DRM could be saturable. Alternative hypothesis is that the re-positioning of myristoyl group may stabilize the Gag-PM association or Gag–Gag interaction, both of which should lead to an increased viral production.

Membrane proteins do not serve as an ideal PM-targeting motif for improvement of the lentiviral vector. The substitution of myr signal with membrane proteins appears to be less favorable because the PM-targeting efficiency of the membrane protein constructs was not high enough to produce VLP, probably because Gag starts to assemble on the ER membrane and bud into intracellular membrane compartments. This premature assembly may block the efficient ER exit of the membrane protein-Gag derivatives. In 293T cells transiently transfected with plasmids expressing membrane Gag mutants, high electron density signals on the intracellular membranes and PM, representing assembled membrane protein-Gag mutants, were observed (data not shown). In addition, intracellular VLP formation was observed in intracellular membrane compartments surrounding the nucleus (data not shown). These observations were consistent with the confocal microscopy data, and suggest that the membrane protein-Gag constructs are assembly-competent. Interestingly, the morphology of the intracellular virion of CXCR4^{DC}-*gag-pol* was similar to late domain-defective HIV-1 particles. These data may imply that the membrane protein-Gag derivatives are not fully competent in VLP formation and/or release.

Considering our data, HIV-1 could have evolved to be able to produce more virus particles than it does now. However, such a virus was not selected in nature. This is presumably because the increased viral production may not confer a strong selective advantage for HIV-1 to spread in human population. It is possible that such a virus may kill the host, resulting in the loss of opportunity to be transmitted to a new host. Alternatively, such a virus may be more immunogenic, thus have selective disadvantage in the host. Conversely, it is possible that HIV-1 has already evolved to bud from its natural target cells, namely CD4-positive T lymphocytes or macrophages. If this is the case, our experimental observation might be only applied to the lentiviral vector production in 293T cells.

Our next generation lentiviral vector should contribute to an increase in lentiviral vector applications, as a tool both for molecular biology research and for human gene therapy. The safety concerns involving Gag amino-terminal modification should be critically examined to use the modified lentiviral vector in clinical trials because the effect of amino-terminal modification of Gag on the lentiviral life cycle is unpredictable. The amino-terminal modification of Gag may alter the chromosomal integration site preference of the lentiviral vector genome. A genome-wide survey to determine the cellular genomic loci in which the Gag-modified lentiviral vector preferentially inserts its genome, compared with the original viral vector, should be conducted. In addition, it may be important to measure the frequency of insertional oncogenesis using small animal models. It is also possible that the fidelity of reverse transcription could be affected by the Gag amino-terminal modification. If the accuracy of reverse transcription drops, the therapeutic effect of the modified lentiviral vector might be affected. These issues should be addressed before the modified lentiviral vector is applied to human gene therapy.

We may be able to further improve the lentiviral vector using systematic modifications of Gag, but such an approach has yet to be examined. For example, the positioning the myr attachment site in all the myr signal Gag derivatives tested in this study was –22 amino acids relative to the original position. A better myristol group-positioning site or other PM-targeting signals to boost viral production and infectivity could be identified by performing an exhaustive systematic modification study.

Materials and methods

Plasmids

The codon optimized HIV-1 *gag* was amplified by PCR from pSyn HIV-1 *gag-pol*[21] using the following primers: HIV-1 *gag* forward 5′-ACCGGTCTCGAGCCACCAT GGGCGCCAGGGCCAGCGTGCTGAGC-3′, HIV-1 *gag* reverse 5′-TCATTGGATCCGGTCGTCATCGTCTTTGT AGTCTTGTGACGAGGGGTCGTTGCCAAAG-3′. The PCR fragment was cloned into pCR4 Blunt TOPO (Invitrogen, Tokyo, Japan), digested with *Xho*I–*Bam*HI, and the resulting fragment was cloned into the *Xho*I–*Bam*HI sites of pEGFP-N2 (Clontech, Palo Alto, CA, USA), generating pGag-GFP. A FLAG epitope tag was encoded at the carboxy-terminus of Gag. The LA-*gag* has been described previously.[14] The *Sna*BI–*Sac*II fragment from pLA-*gag-pol* was cloned into the *Sna*BI–*Sac*I sites of pSyn HIV-1 *gag-pol*, generating the pLA-*gag*-GFP.

The CD4 FL or DC was amplified from CD4 complementary DNA[22] using the following primers: FL and DC forward 5′-GGATCCCGGGCCACCATGAACCG GGGAGTCCCTTTTAGGC-3′, FL reverse 5′-GAATT CAATGGGGCTACATGTCTTCTGAAACCGG-3′, and DC reverse 5′-GAATTCGTGCCGGCACCTGACACAGAAG AAGATGCC-3′. The PCR fragments were cloned into pCR4 Blunt TOPO (Invitrogen), digested with *Bam*HI–*Eco*RI, and the resulting fragments were cloned into the *Bgl*II*Eco*RI sites of pEGFP-N2, generating pCD4$^{FL/DC}$-GFP. The *Sna*BI–*Eco*RI fragments from pCD4$^{FL/DC}$-GFP were cloned into the corresponding sites of pLA-*gag*-GFP, generating pCD4$^{FL/DC}$-*gag*-GFP.

Q1

The full-length human CD8 ORF was amplified by reverse transcriptase-PCR using mRNA isolated from PBMC with following primers: 5′-GCTAGCATGGCCT TACCAGTGAC-3′and 5′-AGATCTATGACGTATCTCGC CGAAAGGCTG-3′. An *Nhe*I–*Bgl*II fragment was cloned into the corresponding sites of pEGFP-N1 (Clontech), generating pEGFPN1hCD8. The *Sna*BI–*Sal*I fragment from pEGFPN1hCD8 was cloned into the *Sna*BI–*Xho*I site of pCXCR4^{FL}-*gag*-GFP, generating pCD8-*gag*-GFP.

The CXCR4 FL and DC were amplified from the CXCR4 complementary DNA[22] using the following primers: FL and DC forward 5′-ACCGGTGCCACCATG GAGGGGATCAGTATATACACTTCAG-3′, FL reverse 5′-AGATCTCGCTGGAGTGAAAACTTGAAGACTCAGA CTC-3′, and DC reverse 5′-AGATCTTGGCTCCAAG GAAAGCATAGAGGATGGG-3′. The *Age*I–*Bgl*II fragments of the PCR products were cloned into *Age*I–*Bgl*II sites of pEGFP-C2, generating pCXCR4$^{FL/DC}$-GFP. The *Sna*BI–*Eco*RI fragments from pCXCR4$^{FL/DC}$-GFP were cloned into the corresponding sites of pLA-*gag*-GFP, generating pCXCR4$^{FL/DC}$-*gag*-GFP.

The following oligonucleotides were annealed and cloned into the BsrGI site of pEGFP-N2 to generate pEGFP-N2-FLAG: 5′-GTACGACTACAAAGACGATGA CGACTATAAGTAAGC-3′ and 5′-GGCCGCTTACTTA TAGTCGTCATCGTCTTTGTAGTC-3′. HIV-1 Env was amplified from pgp160opt that encodes a codon-optimized gp160 (obtained through the NIH AIDS Research and Reference Reagent Program[23]) using the following primers: 5′-GGAACTGGTTCGACATCACCAAGTGGCT GTGG-3′ and 5′-GTTAACCCCGGGATCCAGCAGGGC GGTCTCGAAGCCCTGGCGGATGCGGC-3′. The *Bgl*II–*Xma*I fragment of the PCR product was cloned into pEGFP-N2 flag, generating pgp160opt3fwd2revEGFPN2f. The *Nde*I–*Sfi*I fragment from pgp160opt was cloned into pgp160opt3fwd2revEGFPN2f, generating pgp160optGFPf. The *Afe*I–*Mfe*I fragment carrying *gag*-GFP was cloned into the pgp160optGFPf, generating pEnv-*gag*-GFP.

The PH domain of phospholipase C-δ1 from pGFP-PH (generous gift from Dr Meyer's group,[24]) was amplified using following primers: forward 5′- CGCTAGCACC GGTGCCACCATGGACTCGGGCCGGGACTTCCTG-3′ and reverse 5′- CCTCGAGGCTGGATGTTGAGCTCCTT CAGG-3′. The *Nhe*I–*Xho*I fragment of the PCR product was cloned into the corresponding sites of pLA-*gag*-GFP, generating pPH-*gag*-GFP.

The following oligonucleotides were annealed and inserted into the *Nhe*I–*Xho*I sites of pLA-*gag*-GFP to generate pmyr/pal^{lyn}-*gag*-GFP, pmyr^{lyn}-*gag*-GFP, ppal^{lyn}-*gag*-GFP, pGα (12)-*gag*-GFP, pGα (13)-*gag*-GFP, pGα (16)-*gag*-GFP, pmyr^{MLV}-*gag*-GFP, pmyr^{HIV-1}-*gag*-GFP: myr/pal^{lyn} forward 5′- CTAGCGCCACCATGGGCTGCAT CAAGTCCAAGCGGAAGGACAACTTGAACGACGAC GAGCG-3́ and myr/pal^{lyn} reverse 5′- TCGACGCTC GTCGTCGTTCAAGTTGTCCTTCCGCTTGGACTTGAT GCAGCCCATGGTGGCG-3́; myr^{lyn} forward 5′- CTAGC GCCACCATGGGCGCCATCAAGTCCAAGCGGAAGG ACAACTTGAACGACGACGAGCG-3′ and myr^{lyn} reverse 5′- TCGACGCTCGTCGTCGTTCAAGTTGTCCT TCCGCTTGGACTTGATGGCGCCCATGGTGGCG-3′; pal^{lyn} forward 5′- CTAGCGCCACCATGGCATGTATTAA ATCAAAAAGGAAAGACCg-3′ and pal^{lyn} reverse 5′- TC GACGGTCTTTCCTTTTTGATTTAATACATGCCATGGT GGCG-3′; Gα(12) forward 5′- CTAGCGCCACCATGT CCGGCGTGGTGCGGACCCTGTCCCGGTGCCTGCTG CCCGCCGAAGCCGGCCG-3′ and Gα(12) reverse 5′- TC GACGGCCGGCTTCGGCGGGCAGCAGGCACCGGGA CAGGGTCCGCACCACGCCGGACATGGTGGCG-3′; Gα(13) forward 5′- CTAGCGCCACCATGGCCGACTTC CTGCCCTCCCGGTCCGTGTGCTTCCCCGGCTGCGTG CTGACCAACCG-3′ and Gα(13) reverse 5′- TCGACGG TTGGTCAGCACGCAGCCGGGGAAGCACACGGACCG GGAGGGCAGGAAGTCGGCCATGGTGGCG-3′; Gα(16) forward 5′- CTAGCGCCACCATGGCCCGGTCCCTGCG GTGGCGGTGCTGCCCCTGGTGCCTGACCGAGGACGA GAAGGCCGCCCG-3′ and Gα(16) reverse 5′- TCGAC GGGCGGCCTTCTCGTCCTCGGTCAGGCACCAGGGGC AGCACCGCCACCGCAGGGACCGGGCCATGGTGGC G-3′; myr^{HIV-1} forward 5′- CTAGCGCCACCATGGGCG CCAGGGCCAGCGTGCTGAGCGGCGGCGAGCTGGAC AGGTGGCG-3′ and myr^{HIV-1} reverse 5′- TCGACGC CACCTGTCCAGCTCGCCGCCGCTCAGCACGCTGGCC CTGGCGCCCATGGTGGCG-3′; myr^{MLV} forward 5′- CTA GCGCCACCATGGGCCAGACTGTTACCACTCCCTTAAG TTTGACCTTAGGTCACTGGCG-3′ and myr^{MLV} reverse 5′- TCGACGCCAGTGACCTAAGGTCAAACTTAAGGGA GTGGTAACAGTCTGGCCCATGGTGGCG-3′. The *Sna*a-BI–*Sac*II fragments from pmyr/pal^{lyn}-*gag*-GFP, pmyr^{lyn}-*gag*-GFP, pmyr^{MLV}-*gag*-GFP and pmyr^{HIV-1}-*gag*-GFP were cloned into the corresponding sites of pSyn HIV-1 *gag-pol* to generate pmyr/pal^{lyn}-*gag-pol*, pmyr^{lyn}-*gag-pol*, pmyr^{MLV}-*gag-pol* and pmyr^{HIV-1}-*gag-pol*, respectively.

The following linkers were inserted into the *Bam*HI site of the pGag-GFP, to generate the pHIV-1 *gag*f AB linker: 5′-GATCAAGGATCCACCGGTAGATCTGACCG GTGGATCCTT-3′ and 5′-GATCAAGGATCCACCGGT CAGATCTACCGGTGGATCCTT-3′. The firefly luciferase open reading frame was amplified by PCR using the following primers: 5′-ACCGGTCTCGAGGGCCAC CATGGAAGACGCCAAAAACATAAAGAAAGG-3′ and 5′-GAATTCGGATCCTTACACGGCGATCTTTCCGCCCT TCTTGGCC-3′. The *Age*I–*Eco*RI fragment of the PCR product was cloned into the *Bam*HI site of the pHIV-1 *gag*f AB linker, producing pGag-fLuc. The *Nhe*I–*Xba*I fragment from phRL-CMV (Promega, Tokyo, Japan) was inserted into the *Bam*HI site of pGag-fLuc, generating the pGag-Rluc II, using the following linkers: *Nhe*I side, 5′-GATCTGGTTACCCAATTG-3′ and 5′-CTAGCAATTG GGTAACCA-3′; *Xba*I side, 5′-CTAGCGAATTCA-3′ and 5′-GATCTGAATTCG-3′.

The *Nde*I–*Sac*II fragment from pPH-*gag*-GFP[14] was cloned into the corresponding sites of pGag-Rluc II, generating pPH-*gag*-Rluc. The *Apa*I–*Hpa*I fragments from pmyr/pal^{lyn}-*gag*-GFP, pmyr^{lyn}-*gag*-GFP, pmyr^{MLV}-*gag*-GFP and pmyr^{HIV-1}-*gag*-GFP were cloned into the corresponding sites of pGag-Rluc II, generating pmyr/pal^{lyn}-*gag*-Rluc, pmyr^{lyn}-*gag*-Rluc, pmyr^{MLV}-*gag*-Rluc and pmyr^{HIV-1}-*gag*-Rluc, respectively.

The Vps4DN expression vector was the generous gift of Dr H Gottlinger (University of Massachusetts). Other plasmids including pLenti-luciferase, pVSV-G and pRevpac have been described previously.[14]

Cells and transfection

Cells were maintained in RPMI 1640 medium (Sigma, St Louis, MA, USA) supplemented with 10% fetal bovine serum (Japan Bioserum, Tokyo, Japan), 50 U ml^{-1} penicillin and 50 μg ml^{-1} streptomycin (Invitrogen), at 37 °C in a humidified 5% CO_2 atmosphere. Cells were

transfected with Lipofectamine 2000 according to the manufacturer's protocol (Invitrogen).

Western blotting

Transfected 293FT cells were washed once with Dullbeco's phosphate-buffered saline (Sigma), centrifuged and lysed in a buffer containing 0.31 M Tris-HCl (pH 6.8), 10% (w/v) sodium dodecyl sulfate, 50% (v/v) glycerol, 500 mM dithiothreitol and 0.25% (w/v) bromophenol blue. Proteins were separated by sodium dodecyl sulfate–polyacrylamide gel electrophoresis and transferred to polyvinylidine difluoride membranes (Millipore, Tokyo, Japan). Membranes were incubated with primary antibodies including polyclonal anti-flag (Rockland Immunochemicals, Gilbertsville, PA, USA), anti-$p24^{CA}$ mAb clone 183-H12-5C (NIH AIDS Research and Reference Reagent Program), anti-HIV-1 IN mAb clone ab72007 (Abcam, Cambridge, MA, USA) or anti-Bip mAb clone 40 (BD Biosciences, Tokyo, Japan), followed by a horseradish peroxidase conjugated secondary antibody (Envision, Dako, Tokyo, Japan). Chemiluminescence was generated using Lumilight (Roche, Tokyo, Japan) or Lumigen (GE Healthcare, Tokyo, Japan). Signals were detected using an LAS-3000 mini Lumino-Image analyzer operated by the LAS-300 mini Image Reader software (ver.2.2, Fuji Film, Tokyo, Japan). The brightness and contrast of the image were adjusted using Adobe Photoshop (ver.7.0, Adobe, Tokyo, Japan).

Confocal microscopy

Transfected 293T cells were grown on slide glass in the presence of Hoechst 33258 (Sigma) for 24 h, fixed (4% formaldehyde), mounted and analyzed using confocal fluorescence microscopy (LSM510 Meta 63 × NA 1.4 lens, Carl Zeiss MicroImaging Inc., Tokyo, Japan). The brightness and contrast of the image were adjusted using the LSM image browser (Carl Zeiss).

VLP assay

Transfected 293FT cells were washed once with phosphate-buffered saline, centrifuged and lysed in buffer A (150 mM NaCl, 50 mM Tris-HCL (pH 8.0), 0.5% IGEPAL CA-630) for 0.5–1 h on ice (cell fraction). The cell culture medium was collected, passed through a 0.45 μm filter, and VLP were pelleted by ultracentrifugation (541 k × *g* for 1 h). The VLP pellet was lysed in buffer A for 0.5–1 h (VLP fraction). The green fluorescent intensities of cell and VLP fractions were quantified with a DTX880 Multimode Detector (excitation 485 nm, emission 535 nm) (Beckman Coulter, Tokyo, Japan). The efficiency of VLP production was calculated by dividing the green fluorescent intensity of the VLP fraction by that of the cell fraction.

Infection with lentiviral vector

The 293FT cells grown in six-well plates were transfected with *gag-pol* vector (1 μg), pLenti-luciferase (0.65 μg), pVSV-G (0.4-0.8 μg) or pRevpac (0.05 μg) using Lipofectamine 2000, and replated into three wells of a six-well plate at 4–6 h after transfection. At 48 h after transfection, the cell culture medium was collected, passed through a 0.45 μm filter (Millex-HV polyvinylidine difluoride; Millipore), and mixed with dextran (final concentration 16.25 μg ml^{-1}; DEAE-Dextran chloride, MW ~500 kDa; ICN Biomedicals Inc., Aurora, OH, USA). The 293FT cells at 50% confluency in 24-well plates were exposed to 800 μl of cell culture medium containing viruses. At 4–6 h after infection, 293FT cells were split into 4 wells of a 48-well plate. At 48 h after infection, the luciferase activity was measured using the Steady-Glo Luciferase Assay system (Promega). Luminescence was detected using a Veritas Microplate Luminometer (Promega).

Enzyme-linked immunosorbent assay

A p24 ELISA was conducted according to the manufacturer's protocol (Zeptometrics, Buffalo, NY, USA). To measure cellular p24, transfected 293T cells were washed once with phosphate-buffered saline, lysed in 500 μl buffer A (described above) for 30 min, and subjected to the ELISA.

Bioluminescence resonance energy transfer

The basic protocol for the BRET assay has been described previously.[25] Briefly, 293FT cells grown in a six-well plate were transfected with 0.05–0.2 μg of expression plasmids for Gag derivatives fused to the Rluc together with 1–2 μg of Gag derivatives fused to GFP. At 48 h after transfection, cells were collected and incubated with the Rluc substrate according to the manufacturer's protocol, with the exception that a 5- to 10-fold higher substrate concentration was used (ViviRen Live Cell Substrate; Promega). We measured BRET signals under the conditions in which the GFP and Rluc expression levels were almost similar among the tested samples. The fluorescent and bioluminescent signals were measured using a Tristar LB941 instrument (Berthold Technologies, Bad Wildbad, Germany).

Membrane floatation assay

293FT cells were transfected with a *gag* expression vector using Lipofectamine 2000 (Invitrogen) according to the manufacturer's protocol. At 48 h after transfection, cells were rinsed with ice-cold phosphate-buffered saline and centrifuged at 600 × *g* for 5 min. Cell pellets were resuspended in a buffer containing 10 mM Tris-Cl (pH 7.5), 4 mM EDTA and protease inhibitor cocktail (Sigma), and sonicated on ice. Cell lysates were centrifuged at 370 × *g* for 3 min. A 120 μl aliquot of supernatant was mixed with 3.6 μl 5 M NaCl (final concentration = 150 mM) and 120 μl of TNE-T (100 mM Tris-Cl (pH 7.5), 600 mM NaCl, 16 mM EDTA and 0.5% Triton X-100). These samples were placed on ice for 20 min. Subsequently, 200 μl of supernatant was mixed with 1 ml of 85.5% (wt/vol) sucrose in TNE and placed on the bottom of a centrifuge tube (Ultra Clear, Beckman Coulter), overlayed with 2.8 ml 65% and 1.2 ml 10% (wt/vol) sucrose in TNE, respectively. The gradient Q2 solution was centrifuged for 16 h at 1 48 862 × *g* at 4 °C in a BECKMAN SW55Ti rotor and 10 fractions of 500 μl each were recovered from top-to-bottom.

Transmission electron microscopy (TEM)

Transmission electron microscopy imaging was conducted by Hanaichi Co Ltd (Okazaki, Japan). Transfected 293T cells were removed culture medium, fixed (2% glutaraldehyde, 2% osmium tetroxide), and imaged by transmission electron microscopy (JEOL JEM2000EX Q3 at 100 kV).

Conflict of interest

The authors declare no conflict of interest.

Acknowledgements

This work was supported by the Japan Health Science Foundation, the Japanese Ministry of Health, Labor and Welfare (H18-AIDS-W-003 to JK) and the Japanese Ministry of Education, Culture, Sports, Science and Technology (18689014 and 18659136 to JK).

References

1 MacGregor RR. Clinical protocol. A phase 1 open-label clinical trial of the safety and tolerability of single escalating doses of autologous CD4T cells transduced with VRX496 in HIV-positive subjects. *Hum Gene Ther* 2001; **12**: 2028–2029.
2 Hofling AA, Devine S, Vogler C, Sands MS. Human CD34+ hematopoietic progenitor cell-directed lentiviral-mediated gene therapy in a xenotransplantation model of lysosomal storage disease. *Mol Ther* 2004; **9**: 856–865.
3 Bank A, Dorazio R, Leboulch P. A phase I/II clinical trial of beta-globin gene therapy for beta-thalassemia. *Ann NY Acad Sci* 2005; **1054**: 308–316.
4 Manilla P, Rebello T, Afable C, Lu X, Slepushkin V, Humeau LM *et al.* Regulatory considerations for novel gene therapy products: a review of the process leading to the first clinical lentiviral vector. *Hum Gene Ther* 2005; **16**: 17–25.
5 Cockrell AS, Kafri T. Gene delivery by lentivirus vectors. *Mol Biotechnol* 2007; **36**: 184–204.
6 Lundberg C, Björklund T, Carlsson T, Jakobsson J, Hantraye P, Déglon N *et al.* Applications of lentiviral vectors for biology and gene therapy of neurological disorders. *Curr Gene Ther* 2008; **8**: 461–473.
7 Maetzig T, Galla M, Brugman MH, Loew R, Baum C, Schambach A. Mechanisms controlling titer and expression of bidirectional lentiviral and gammaretroviral vectors. *Gene Ther* 2010; **17**: 400 .
8 ter Brake O, Berkhout B. Lentiviral vectors that carry anti-HIV shRNAs: problems and solutions. *J Gene Med* 2007; **9**: 743–750.
9 McCart JA, Bartlett DI. Lentiviral vectors. In: Templeton NS (ed). *Gene and Cell Therapy: Therapeutic Mechanisms and Strategies*, rd edn CRC Press: Carrollton, 2008, pp 245–262.
10 Fiorentini S, Marini E, Caracciolo S, Caruso A. Functions of the HIV-1 matrix protein p17. *New Microbiol* 2006; **29**: 1–10.
11 Hearps AC, Jans DA. Regulating the functions of the HIV-1 matrix protein. *AIDS Res Hum Retroviruses* 2007; **23**: 341–346.
12 Bukrinskaya A. HIV-1 matrix protein: a mysterious regulator of the viral life cycle. *Virus Res* 2007; **124**: 1 .
13 Klein KC, Reed JC, Lingappa JR. Intracellular destinies: degradation, targeting, assembly, and endocytosis of HIV Gag. *AIDS Rev* 2007; **9**: 150–161.
14 Urano E, Aoki T, Futahashi Y, Murakami T, Morikawa Y, Yamamoto N *et al.* Substitution of the myristoylation signal of human immunodeficiency virus type 1 Pr55Gag with the phospholipase C-delta1 pleckstrin homology domain results in infectious pseudovirion production. *J Gen Virol* 2008; **89**: 3144–3149.
15 Garrus JE, von Schwedler UK, Pornillos OW, Morham SG, Zavitz KH, Wang HE *et al.* Tsg101 and the vacuolar protein sorting pathway are essential for HIV-1 budding. *Cell* 2001; **107**: 55–65.
16 Lindwasser OW, Resh MD. Multimerization of human immunodeficiency virus type 1 Gag promotes its localization to barges, raft-like membrane microdomains. *J Virol* 2001; **75**: 7913–7924.
17 Ono A, Freed EO. Plasma membrane rafts play a critical role in HIV-1 assembly and release. *Proc Natl Acad Sci USA* 2001; **98**: 13925–13930.
18 Ono A, Freed EO. Binding of human immunodeficiency virus type 1 Gag to membrane: role of the matrix amino terminus. *J Virol* 1999; **73**: 4136–4144.
19 Gottlinger HG, Sodroski JG, Haseltine WA. Role of capsid precursor processing and myristoylation in morphogenesis and infectivity of human immunodeficiency virus type 1. *Proc Natl Acad Sci USA* 1989; **86**: 5781–5785.
20 Zhou W, Resh MD. Differential membrane binding of the human immunodeficiency virus type 1 matrix protein. *J Virol* 1996; **70**: 8540–8548.
21 Wagner R, Graf M, Bieler K, Wolf H, Grunwald T, Foley P *et al.* Rev-independent expression of synthetic gag-pol genes of human immunodeficiency virus type 1 and simian immunodeficiency virus: implications for the safety of lentiviral vectors. *Hum Gene Ther* 2000; **11**: 2403–2413.
22 Komano J, Miyauchi K, Matsuda Z, Yamamoto N. Inhibiting the Arp2/3 complex limits infection of both intracellular mature vaccinia virus and primate lentiviruses. *Mol Biol Cell* 2004; **15**: 5197–5207.
23 Gao F, Li Y, Decker JM, Peyerl FW, Bibollet-Ruche F, Rodenburg CM *et al.* Codon usage optimization of HIV type 1 subtype C gag, pol, env, and nef genes: *in vitro* expression and immune responses in DNA-vaccinated mice. *AIDS Res Hum Retroviruses* 2003; **19**: 817–823.
24 Stauffer TP, Ahn S, Meyer T. Receptor-induced transient reduction in plasma membrane PtdIns(4,5)P2 concentration monitored in living cells. *Curr Biol* 1998; **8**: 343–346.
25 Hamatake M, Aoki T, Futahashi Y, Urano E, Yamamoto N, Komano J. Ligand-independent higher-order multimerization of CXCR4, a G-protein-coupled chemokine receptor involved in targeted metastasis. *Cancer Sci* 2009; **100**: 95 .

 DOI 10.1002/eji.200939479 Eur. J. Immunol. 2010. 40: 1504–1509

European Journal of Immunology

SHORT COMMUNICATION

Inhibition of HIV replication by a CD4-reactive Fab of an IgM clone isolated from a healthy HIV-seronegative individual

Makiko Hamatake[1], Jun Komano[1], Emiko Urano[1], Fumiko Maeda[2], Yasuko Nagatsuka[3] and Masataka Takekoshi[2]

[1] AIDS Research Center, National Institute of Infectious Diseases, Tokyo, Japan
[2] Department of Molecular Life Science, Division of Basic Molecular Science and Molecular Medicine, Tokai University School of Medicine, Isehara, Japan
[3] Laboratory for Molecular Membrane Neuroscience, Brain Science Institute, RIKEN, Wako, Saitama, Japan

HIV replication is restricted by some anti-CD4 mouse mAb *in vitro* and *in vivo*. However, a human monoclonal anti-CD4 Ab has not been isolated. We screened EBV-transformed peripheral B cells from 12 adult donors for CD4-reactive Ab production followed by functional reconstitution of Fab genes. Three independent IgM Fab clones reactive specifically to CD4 were isolated from a healthy HIV-seronegative adult (~0.0013% of the peripheral B cells). The germ line combinations for the V_H and V_L genes were V_H3-33/$_L6$, V_H3-33/$_L12$, and V_H4-4/$_L12$, respectively, accompanied by somatic hypermutations. Genetic analysis revealed a preference for V-gene usage to develop CD4-reactive Ab. Notably, one of the CD4-reactive clones, HO538-213, with an 1×10^{-8}M dissociation constant (Kd) to recombinant human CD4, limited the replication of R5-tropic and X4-tropic HIV-1 strains at 1–2.5 μg/mL in primary mononuclear cells. This is the first clonal genetic analysis of human monoclonal CD4-reactive Ab. A mAb against CD4 isolated from a healthy individual could be useful in the intervention of HIV/AIDS.

Key words: Autoimmunity · CD4-reactive Ab · IgM · Inhibition of HIV replication

Supporting Information available online

Introduction

CD4 is a T-cell marker that serves as a principal receptor for HIV. CD4-reactive Ab are detected in HIV-infected individuals (~13%) [1, 2] and HIV-exposed seronegative individuals (34%) [3]. In addition, some healthy individuals are positive for anti-CD4 Ab (~0.6%) [4]. Replication of multiple HIV clades is blocked by mouse mAb against CD4 *in vitro* and *in vivo* [5–12]. Thus, it is possible that anti-CD4 Ab play a role in protecting individuals from HIV infection and delaying AIDS disease progression. Similar arguments have been made for Ab against CCR5, a coreceptor for HIV [3, 10, 13]. Furthermore, some clinical studies suggest that CD4-reactive Ab, including a humanized mAb, has therapeutic potential against HIV infection and AIDS progression [5, 8, 10, 12]. However, the development and pathophysiological roles of self-recognizing Ab in healthy individuals are still largely unknown, and a human mAb against CD4 has not yet been isolated.

To gain insights into the genesis of auto-reactive Ab and to characterize the nature of CD4-reactive auto-Ab, we conducted experiments to isolate human monoclonal anti-CD4 Ab from PBMC of 12 HIV-seronegative adult donors. We succeeded in isolating

Correspondence: Dr. Jun Komano
e-mail: ajkomano@nih.go.jp

three independent IgM clones recognizing CD4 from a healthy donor. Analysis of the V-region sequences of CD4-reactive Ab revealed a preference for V gene usage to give rise to CD4-reactive Ab. This is the first report describing CD4-reactive human mAb.

Results and discussion

Isolation of CD4-reactive IgM clones from a healthy individual

PBMC were collected from 12 HIV-seronegative adult volunteers, including two healthy and ten with autoimmune disorders, and B-lymphoblastoid cell lines (B-LCL) were established by infecting the cells with EBV (for experimental procedure, see Supporting Information Fig. 1). B-LCL were propagated in oligoclonal pools. In 790 cultures from one healthy donor, we identified two cultures positive for recombinant human CD4 (rhCD4) reactivity, HO538 and HO702, using ELISA (Fig. 1A). This donor may have a unique Ab repertoire, as auto-reactive B-LCL cultures were identified significantly more frequently in this donor than in the others (Fig. 1A). The rhCD4 reactivity was specific, as no binding was observed to 72 other viral, bacterial, and auto-Ag screened in parallel (Supporting Information Fig. 2). We amplified the Ig genes encoding the Fab regions by RT-PCR and cloned them into the bacterial expression vector pFabI-His2 that produces Fab fragments of an inserted set of V_H and V_L genes. We expected that some clones should reconstitute the CD4-reactive Fab present in the original B-LCL cultures. After screening by ELISA, one CD4-reactive Fab clone, HO538-213, was isolated from the HO538 culture, and two independent clones, HO702-001 and HO702-016, were isolated from the HO702 culture. These Fab clones originated from IgM, as determined by the sequence analysis. The estimated efficiency of peripheral B cells producing CD4-reactive Ab was ~0.0013% (three clones/2.4×10^5 estimated screened B cells × 100 (%), given that the B cells compose 10% of PBMC and that EBV immortalization is 30% efficient on average) [14]. According to the ELISA data, the Fab concentrations that yielded 50% maximal binding were ~8 μg/mL for HO538-213, and ~1 μg/mL for HO702-001 and HO702-016 (Fig. 1B). Consistent with these data, the BIACORE assay revealed that the dissociation constant (Kd) of HO538-213, HO702-001, and HO702-016 to rhCD4 was 6.5×10^{-8}, 7.7×10^{-9}, and 2.7×10^{-9} M, respectively (Fig. 1C), which is relatively weak compared with average Ab–Ag interactions (*e.g.* the Kd of mouse mAb Leu-3a to rhCD4 is 2.2×10^{-10} M).

Genetic analysis of CD4-reactive IgM clones

The Fab sequences were analyzed by the Kabat database (http://www.ncbi.nlm.nih.gov/igblast/) in GenBank, as previously described [15, 16]. The Ig gene family of each gene and the most homologous germline are indicated (Fig. 2A). All the three clones were of the IgM class and had a κ-chain for V_L. Comparison of the

A

Donor	Number of tested cultures	CD4	Nuclear antigen	Blood type i-glycolipid
Healthy 1	790	2 (0.3%)*	21 (2.6%)*	28 (3.5%)*
Healthy 2	160	0	0	0
Autoimmune (10 individuals)	435	0	3 (0.7%)	0

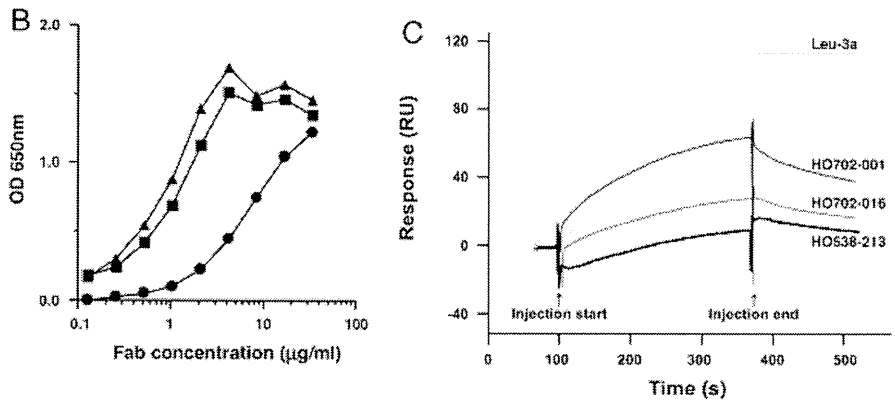

Figure 1. Isolation and characterization of healthy human-derived CD4-reactive Ab. (A) Summary of the frequency of B-LCL cultures that reacted with representative auto-Ag. The number of cultures positive for rhCD4 reactivity, HeLa cell nuclear staining, and blood type i-glycolipid are shown. *$p<0.05$, compared with other donor groups, Fisher's exact test. (B) CD4-binding kinetics of CD4-reactive IgM Fab. Serial dilutions of HO538-213 (circles), HO702-001 (triangles), and HO702-016 (squares) were incubated in microtiter plates pre-coated with rhCD4. (C) Surface plasmon resonance analysis of CD4-reactive IgM FAb HO702-001 (black), HO702-016 (dark gray), HO538-213 (bold), and mAb Leu-3a (gray) binding to immobilized rhCD4. The concentration of Ab was 0.3 μg/mL, flow rate 20 μL/min, and reaction time 270 s. RU, resonance units.

heavy chain with the germlines revealed that the μ-chains of HO538-213 and HO702-001 were 95 and 97% homologous to germ line V_H3-33, respectively, while HO702-016 was 96% homologous to germline V_H4-4 [17]. For the light chains, the κ-chain Vkappa3 of HO538-213 was 97% homologous to germline L6 [6, 18, 19], and κ-chain Vkappa1 of both HO702-001 and HO702-016 was 97% homologous to the germline L12 [6, 18, 19]. These data suggest that there is a preferential use of V_H and V_L genes to develop CD4-reactive Ab, considering the number of V_H and V_L genes present before the Ig gene rearrangement. According to the sequence analysis, the V_H amino acid sequences of HO538-213 and HO702-001 carried distinct mutations, although both were derived from the same germline V_H3-33. The mutations were more frequent in the CDR regions (Fig. 2B and C, Supporting Information Fig. 3), which is characteristic of somatic hypermutation (SHM) associated with affinity maturation. Unlike most SHM, however, mutations involving G/C were not dominant.

A

Clone	Ig class	VH family	Closest germline	% identity	VL family	Closest germline	% identity
HO538-213	IgM	VH 3	VH3-33	95%	Vk3	L6	97%
HO702-001	IgM	VH 3	VH3-33	97%	Vk-1	L12	97%
HO702-016	IgM	VH 4	VH4-4	96%	Vk-1	L12	97%

B

Clone			Number of mutations associated with: A	G	C	T	Ins	Del	GC involvement (%)	Total	aa changes	(%)
HO702-001	heavy chain	FR	3	2	1	0	0	0	50.0	6	2	33.3
		CDR	0	0	0	0	0	0	0.0	5	0	0.0
	light chain	FR	0	0	0	2	0	0	0.0	2	1	50.0
		CDR	1	0	0	0	0	0	0.0	7	0	0.0
		Total	4	2	1	2	11	0	33.3	20	3	15.0
HO702-016	heavy chain	FR	1	0	0	0	0	0	0.0	1	0	0.0
		CDR	0	2	1	0	11	0	100.0	6	0	0.0
	light chain	FR	0	0	0	2	0	0	0.0	2	1	50.0
		CDR	1	0	0	0	6	0	0.0	7	0	0.0
		Total	2	2	1	2	17	0	40.0	24	1	4.2
HO538-213	heavy chain	FR	2	1	1	4	0	0	25.0	8	3	37.5
		CDR	2	2	5	1	15	0	70.0	25	5	20.0
	light chain	FR	1	2	1	0	0	0	75.0	4	3	75.0
		CDR	3	1	0	0	2	0	25.0	6	3	50.0
		Total	8	6	7	6	17	0	50.0	43	13	30.2

C

Light chain

```
                    FR1                          CDR1          FR2           CDR2
HO538-213   EIVMTQSPATLSLSPGERATLSC  RASQSVNNYLA  WYQQKPGQAPSLLIY  DASNRAT
HO702-001/016 D-QL----S---A-V-D-V-IT-  -----ISSH--  ----K--K--K----  K--SLES

                    FR3                          CDR3          FR4
HO538-213   GIPARFSGSGSGTDFTLTISSLEPEDFAVYYC  QQ.RG.WPFHT  FGQGTKLEIKRT
HO702-001/016 -V-S----------E---------Q-D---Y---  --YNSYSRTY-  ------------
```

Heavy chain

```
                    FR1                          CDR1          FR2           CDR2
HO538-213   QVQLVQSGGGVVQPGRSLRLSCA.ASG.FTFS  SYGMH  WVRQAPGKGLEWVA  VVCYDGRTTYYADSVKG
HO702-001   ----QEW-------------------------  -----  --------------  -IN---SNK---------
HO702-016   ----QE--P-L-K-SQT-S-T-TVSG-SISSG  --YWS  -I--PA------IG  .RI-TSGS-N-NP-L-S

                    FR3                          CDR3          FR4
HO538-213   RFTISRDISENTLYLQMNSLRAEDTAVYYCAK  DLNKGYCNNGGCYG.VDC  WGQGTLVTVSS
HO702-001   -------N-K-----------------------R  -..RD.-SG-S--SWF-P  ----------
HO702-016   -V--SV-T-K-QFS-KLS-VT-A--------R  T.-PTL.GR-L.F...-Y  ----------
```

Figure 2. Genetic analysis of CD4-reactive Ab. (A) Summary of the Ig class, V-gene family, closest germ line, and percentage identity of the closest germ line of CD4-reactive Ab. (B) The mutation profiles of the CD4-reactive IgM Fab fragments. (C) The deduced protein sequences of the V_H and V_L genes of the CD4-reactive Fab fragments are aligned. FR, framework region. Dashes and dots indicate identical residues and deletions, respectively. See Supporting Information Fig. 2 for further detail.

Inhibition of HIV replication by a Fab fragment of a CD4-reactive IgM

We next examined the potential impact of these CD4-reactive Fab Ab on HIV replication. Viral replication was monitored in PBMC by measuring $p24^{CA}$ viral Ag levels in the culture supernatant. Among the three IgM Fab clones, HO538-213 suppressed R5-tropic virus HIV-1_{JR-FL} replication by 3.5±1.5-fold at 1–2.5 μg/mL (average±SD from four independent experiments, Fig. 3A). There was a modest but consistent suppression of X4-tropic virus HIV-1_{HXB2} replication (1.4±0.2-fold, average±SD from three independent experiments). BIACORE and ELISA revealed that HO538-213 did not compete with the anti-CD4 mAb Leu-3a [20, 21] for CD4 binding. Leu-3a restricts HIV-1 replication by physically blocking the *Env*-CD4 interaction (data not shown), suggesting that the epitope recognized by HO538-213 is distinct from the *Env*-interacting domain of CD4 [7, 22, 23]. The monoclonal anti-CD4 Ab OKT4a does not block the *Env*-CD4 interaction, but restricts HIV-1 infection, although decreasing CD4 lateral diffusion on the cell surface [24–26]. We hypothesized that HO538-213 may have a similar mechanism of action. CD4 localizes to lipid rafts, and CD4-crosslinking activates signal transduction involving tyrosine kinases [27–29]. Thus, we treated MOLT-4 cells with HO538-213, and the lipid raft fraction was isolated by a membrane floatation assay as verified by the raft markers glycosphingomyelin 1 and sphingomyelin (Fig. 3B, left panel). Tyrosine kinase activitiy was examined by immunoblotting the lipid raft fractions using a PY20 anti-phosphotyrosine mAb (Fig. 3B, right panel, arrowhead). We detected a significant amount of tyrosine phosphorylation in the lipid raft fraction after HO538-213 treatment, indicating that HO538-213 can assemble cell surface CD4. This is consistent with our hypothesis that HO538-213 inhibits HIV-1 infection by decreasing the lateral movement of cell surface CD4.

Does CD4-reactive IgM function as a natural HIV resistance factor?

We then further characterized the donor from which the CD4-reactive Ab was isolated. The donor serum did not show a strong reactivity to rhCD4 at 1:10 dilution, where the non-specific effect was no longer detected. We analyzed the HIV-inhibition titer of the donor plasma. In a TZM-bl cell assay, the plasma did not block HIV replication at 1:50 dilution (data not shown). These data suggest that the CD4-reactive IgM circulates at very low titers in the donor and may not be sufficient to block HIV infection *in vitro*. However, it is possible that the CD4-reactive IgM may be able to limit HIV-1 propagation under *in vivo* conditions.

We next investigated the immunological status of the donor. IgG and IgM levels were within the normal range, and the plasma was negative for rheumatoid factor, anti-DNA, and anti-ribonucleoprotein Ab. However, the donor serum reacted to nuclear Ag at a titer of 1:160 (1:40 or less is considered normal), and the staining patterns were nucleolar (1:160) and speckled (1:80). Consistent with these data, the frequency of auto-reactive

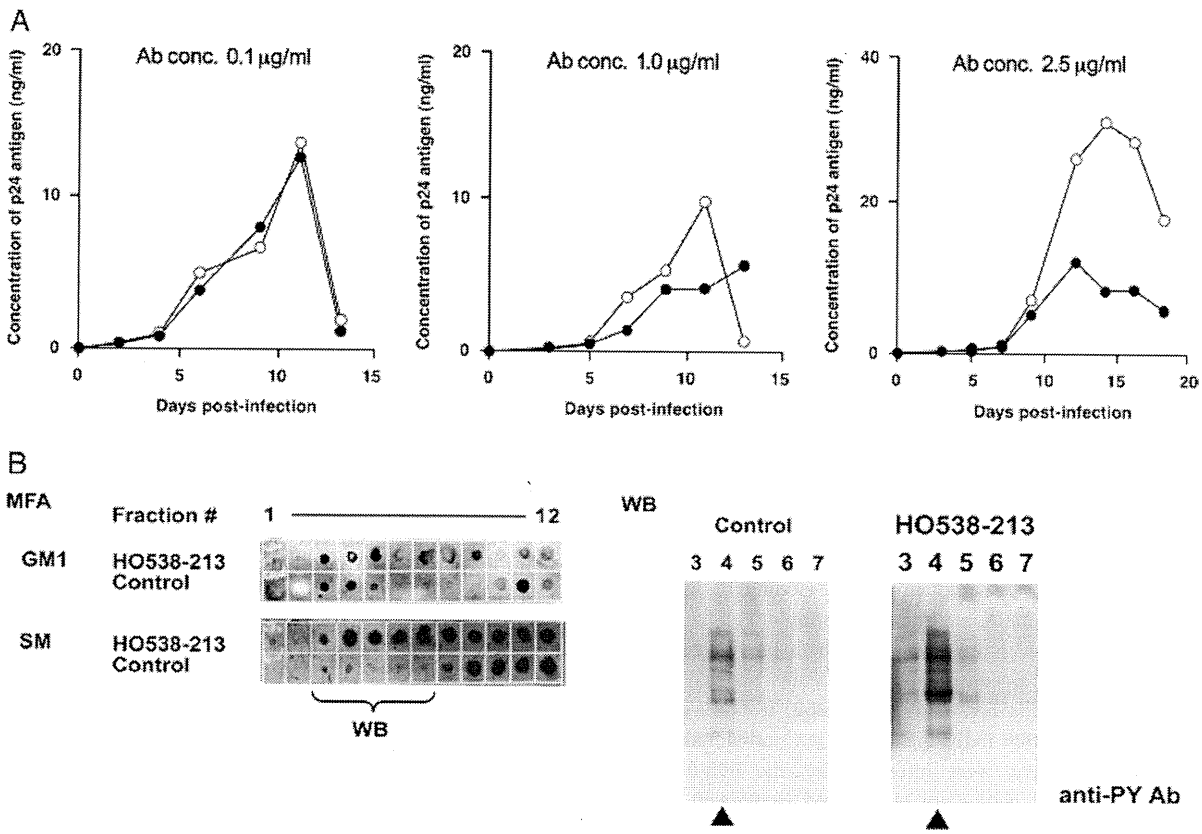

Figure 3. The effect of CD4-reactive Fab clone HO538-213 on HIV-1 replication. (A) The Fab clone HO538-213 (filled circles) was tested for its ability to inhibit HIV-1_{JR-FL} replication at a concentration of 0.1 (left), 1.0 (middle), and 2.5 (right) μg/mL. The CD4 non-reactive Fab clone 13-3 (open circles) was used as a negative control. Representative data from four independent experiments are shown. (B) Activation of the tyrosine kinase signaling cascade by HO538-213 in MOLT-4 cells. The detergent-resistant membrane fraction (arrowhead) was isolated by a membrane floatation assay (MFA) from MOLT-4 cells treated with HO538-213, and phosphotyrosine levels were examined by immunoblotting. GM1, glycosphingomyclin 1; SM, sphingomyelin.

Ab-producing cells from the same donor, namely against nuclear Ag and blood group i-glycolipid, was significantly higher than the other donors (Fig. 1A). In addition, we isolated anti-TNF-α IgG and IgM clones from this donor [16]. Although clinical manifestations of autoimmune disorders were lacking, it is likely that the donor may have an immunological background that generates auto-reactive Ab and tolerates them. Moreover, the donor has been healthy for 29 years, at the time the CD4-reactive Ab was first isolated, suggesting that such CD4-reactive Ab may not disturb host immunity.

Considering that the IgM-producing B cells we isolated went through positive/negative selection, their original target should not be CD4. It is thus likely that the IgM genes accumulated SHM that resulted in cross-reactivity to CD4 in the periphery after B-cell maturation. To better understand the unique immunological features of individuals with CD4-reactive Ab and their auto-reactive Ab repertoire, more human monoclonal self-reactive Ab are needed to analyze both their V-region sequences and cross-reactivities. Our experimental approach might be useful for addressing these issues. Unfortunately, however, we were unable to characterize the CD4-reactive Ab-producing cells, as the oligoclonal cultures of B-LCL were terminated after RNA extraction for our Ig gene cloning strategy. We speculate that B-1 cells could be the source of the CD4-reactive Ab, because B-1 cells produce IgM that often cross-reacts with auto-Ag.

Our genetic data indicated that only a fraction of the CD4-reactive Ab could have some HIV-inhibitory function. It is an open question whether such CD4-reactive HIV-inhibitory Ab may be present in the other healthy individuals, as well as in HIV-seropositive long-term non-progressors.

HIV-inhibitory CD4-reactive Ab are effective against multiple HIV clades, as CD4 is the major HIV receptor for all the viral clades [11]. A clinical trial is being conducted to examine the therapeutic efficacy of a humanized CD4-reactive mAb in patients with HIV infection [8, 12]. Although CD4-reactive Ab can be detected in healthy individuals, safety is always a concern when using self-recognizing Ab as therapeutic drugs. Given that HO538-213 was isolated from a healthy individual and that it recognized a different epitope than Leu-3a, HO538-213 might effectively inhibit HIV without disturbing $CD4^+$ T-cell functions. As noted above, the donor from which the three CD4-reactive IgM Fab were isolated has been healthy for more than 29 years since PBMC collection, suggesting that these Ab may not seriously inhibit $CD4^+$ T-cell functions *in vivo* and thus may be useful in treating HIV infection and other disorders [4].

Concluding remarks

This report provides the first clonal genetic analyses of human monoclonal anti-CD4 Ab. IgM is considered to function in "natural humoral immunity", as it has a relatively low affinity for pathogens and confers natural resistance to infectious agents. However, the pathogen-specific immunity function of IgM has not been demonstrated at a clonal level. Our data suggest that CD4-reactive IgM is present in healthy individuals and can contribute to natural resistance to HIV infection and AIDS progression. This is the first clear demonstration of a natural humoral immunity function of IgM against HIV.

Materials and methods

Functional cloning of heavy and light chain Ab genes

The establishment of Ab-producing cells, cloning of Ig genes encoding V regions, ELISA, and the purification of Fab fragments from *Escherichia coli* have been described previously [16]. The experimental procedure is schematically shown in the Supporting Information Fig. 1. In brief, PBMC from 12 donors, including two healthy individuals and ten individuals with autoimmune disorders, were infected with the B95-8 strain of EBV, and 1×10^4 cells were propagated in 96-well plates. The supernatant was analyzed by ELISA using rhCD4 derived from a baculovirus system (50 ng/well; INTRACELL) as an Ag. Other Ag tested, including viral, bacterial, and auto-Ag, are listed in the Supporting Information Fig. 2. Total cellular RNA was isolated from oligoclonal cell populations positive for anti-CD4 Ab production (RNeasy mini kit, Qiagen). cDNAs were synthesized and amplified by PCR with specific primers for human Ig μ-, γ-, λ-, and κ-chains. Only the μ- and κ-chains were amplified from HO538 and HO702 cultures and cloned into the pFab1-His2 vector, generating bacterial Fab-expression libraries [30]. The pFab libraries were screened for the production of CD4-reactive Fab by ELISA. The Fab fragments were purified using an anti-Fab Ab affinity column. The eluted Fab was dialyzed against PBS and concentrated by centrifugation (VIVASPIN concentrator, Vivascience AG). The purity of the Fab Ab was greater than 95% as determined by SDS-PAGE analysis (data not shown).

Surface plasmon resonance biosensor analysis

Surface plasmon resonance analyses were performed using BIACORE 3000 (GE Healthcare). The hrCD4 was immobilized onto CM5 sensor chips using standard amine-coupling chemistry. The purified Fab was diluted in a running buffer (10 mM HEPES, 0.15 M NaCL, 3 mM EDTA, surfactant P 20, pH 7.4) to 0.3–20 μg/mL and injected at a rate of 20–30 μL/min. The Fab was allowed to associate and dissociate for 120–270 s.

Cells

B-LCL and 293 T cells were maintained in Roswell Park Memorial Institute (RPMI) 1640 (Sigma) supplemented with 10% fetal bovine serum (Japan Bioserum), penicillin, and streptomycin (Invitrogen). The primary mononuclear cells were maintained in RPMI 1640 supplemented with 10% fetal bovine serum, penicillin, streptomycin, 5 μg/mL plasmocin (InvivoGen), 10 mM HEPES, 5 μg/mL anti-CD3 mAb (OKT3, Janssen Pharmaceutical), 70 U/mL recombinant human IL-2 (Shionogi Pharmaceutical), GlutaMax-I (Invitrogen), insulin–transferrin–selenium-A (Invitrogen), and 10 mM HEPES (Invitrogen). Cells were incubated at 37°C in a humidified 5% CO_2 atmosphere.

Other experimental procedures

Procedures for monitoring HIV-1 replication [31] and membrane floatation assays [32] were described previously. Standard auto-Ab was tested by the clinical laboratory testing service SRL (Tokyo, Japan).

Acknowledgements: The authors thank Hideo Tsukamoto for BIACORE analysis. This work was supported by the Japan Health Science Foundation, the Japanese Ministry of Health, Labor and Welfare (H18-AIDS-W-003 to JK), and the Japanese Ministry of Education, Culture, Sports, Science and Technology (18689014 and 18659136 to JK).

Conflict of interest: The authors declare no financial or commercial conflict of interest.

References

1 **Henriksson, G., Manthorpe, R. and Bredberg, A.,** Antibodies to CD4 in primary Sjogren's syndrome. *Rheumatology (Oxford)* 2000. **39**: 142–147.

2 **Lenert, P., Lenert, G. and Senecal, J. L.,** CD4-reactive antibodies in systemic lupus erythematosus. *Hum. Immunol.* 1996. **49**: 38–48.

3 **Lopalco, L., Magnani, Z., Confetti, C., Brianza, M., Saracco, A., Ferraris, G., Lillo, F. et al.,** Anti-CD4 antibodies in exposed seronegative adults and in newborns of HIV type 1-seropositive mothers: a follow-up study. *AIDS Res. Hum. Retroviruses* 1999. **15**: 1079–1085.

4 **Herzog, C., Walker, C., Muller, W., Rieber, P., Reiter, C., Riethmuller, G., Wassmer, P. et al.,** Anti-CD4 antibody treatment of patients with rheumatoid arthritis: I. Effect on clinical course and circulating T cells. *J. Autoimmun.* 1989. **2**: 627–642.

5 **Rieber, E. P., Federle, C., Reiter, C., Krauss, S., Gurtler, L., Eberle, J., Deinhardt, F. and Riethmuller, G.,** The monoclonal CD4 antibody M-T413 inhibits cellular infection with human immunodeficiency virus after viral attachment to the cell membrane: an approach to postexposure prophylaxis. *Proc. Natl. Acad. Sci. USA* 1992. **89**: 10792–10796.

6 Bentley, D. L. and Rabbits, T. H., Human immunoglobulin variable region genes – DNA sequences of two V kappa genes and a pseudogene. *Nature* 1980. **288**: 730–733.

7 Moir, S., Lapointe, R., Malaspina, A., Ostrowski, M., Cole, C. E., Chun, T. W., Adelsberger, J. *et al.*, CD40-Mediated induction of CD4 and CXCR4 on B lymphocytes correlates with restricted susceptibility to human immunodeficiency virus type 1 infection: potential role of B lymphocytes as a viral reservoir. *J. Virol.* 1999. **73**: 7972–7980.

8 Kuritzkes, D. R., Jacobson, J., Powderly, W. G., Godofsky, E., DeJesus, E., Haas, F., Reimann, K. A. *et al.*, Antiretroviral activity of the anti-CD4 monoclonal antibody TNX-355 in patients infected with HIV type 1. *J. Infect. Dis.* 2004. **189**: 286–291.

9 Burastero, S. E., Gaffi, D., Lopalco, L., Tambussi, G., Borgonovo, B., De Santis, C., Abecasis, C. *et al.*, Autoantibodies to CD4 in HIV type 1-exposed seronegative individuals. *AIDS Res. Hum. Retroviruses* 1996. **12**: 273–280.

10 Boon, L., Holland, B., Gordon, W., Liu, P., Shiau, F., Shanahan, W., Reimann, K. A. and Fung, M., Development of anti-CD4 MAb hu5A8 for treatment of HIV-1 infection: preclinical assessment in non-human primates. *Toxicology* 2002. **172**: 191–203.

11 Shearer, M. H., Timanus, D. K., Benton, P. A., Lee, D. R. and Kennedy, R. C., Cross-clade inhibition of human immunodeficiency virus type 1 primary isolates by monoclonal anti-CD4. *J. Infect. Dis.* 1998. **177**: 1727–1729.

12 Hurez, V., Kaveri, S. V., Mouhoub, A., Dietrich, G., Mani, J. C., Klatzmann, D. and Kazatchkine, M. D., Anti-CD4 activity of normal human immunoglobulin G for therapeutic use. (Intravenous immunoglobulin, IVIg). *Ther. Immunol.* 1994. **1**: 269–277.

13 Bomsel, M., Pastori, C., Tudor, D., Alberti, C., Garcia, S., Ferrari, D., Lazzarin, A. and Lopalco, L., Natural mucosal antibodies reactive with first extracellular loop of CCR5 inhibit HIV-1 transport across human epithelial cells. *AIDS* 2007. **21**: 13–22.

14 Sugden, B. and Mark, W., Clonal transformation of adult human leukocytes by Epstein–Barr virus. *J. Virol.* 1977. **23**: 503–508.

15 Takekoshi, M., Maeda, F., Tachibana, H., Inoko, H., Kato, S., Takakura, I., Kenjyo, T. *et al.*, Human monoclonal anti-HCMV neutralizing antibody from phage display libraries. *J. Virol. Methods* 1998. **74**: 89–98.

16 Takekoshi, M., Maeda, F., Nagatsuka, Y., Aotsuka, S., Ono, Y. and Ihara, S., Cloning and expression of human anti-tumor necrosis factor-alpha monoclonal antibodies from Epstein–Barr virus transformed oligoclonal libraries. *J. Biochem.* 2001. **130**: 299–303.

17 Matsuda, F., Ishii, K., Bourvagnet, P., Kuma, K., Hayashida, H., Miyata, T. and Honjo, T., The complete nucleotide sequence of the human immunoglobulin heavy chain variable region locus. *J. Exp. Med.* 1998. **188**: 2151–2162.

18 Huber, C., Schable, K. F., Huber, E., Klein, R., Meindl, A., Thiebe, R., Lamm, R. and Zachau, H. G., The V kappa genes of the L regions and the repertoire of V kappa gene sequences in the human germ line. *Eur. J. Immunol.* 1993. **23**: 2868–2875.

19 Pech, M. and Zachau, H. G., Immunoglobulin genes of different subgroups are interdigitated within the VK locus. *Nucleic Acids Res.* 1984. **12**: 9229–9236.

20 Healey, D., Dianda, L., Moore, J. P., McDougal, J. S., Moore, M. J., Estess, P., Buck, D. *et al.*, Novel anti-CD4 monoclonal antibodies separate human immunodeficiency virus infection and fusion of CD4+ cells from virus binding. *J. Exp. Med.* 1990. **172**: 1233–1242.

21 Peterson, A. and Seed, B., Genetic analysis of monoclonal antibody and HIV binding sites on the human lymphocyte antigen CD4. *Cell* 1988. **54**: 65–72.

22 Benkirane, M., Hirn, M., Carriere, D. and Devaux, C., Functional epitope analysis of the human CD4 molecule: antibodies that inhibit human immunodeficiency virus type 1 gene expression bind to the immunoglobulin CDR3-like region of CD4. *J. Virol.* 1995. **69**: 6898–6903.

23 Sattentau, Q. J., Dalgleish, A. G., Weiss, R. A. and Beverley, P. C., Epitopes of the CD4 antigen and HIV infection. *Science* 1986. **234**: 1120–1123.

24 Pal, R., Nair, B. C., Hoke, G. M., Sarngadharan, M. G. and Edidin, M., Lateral diffusion of CD4 on the surface of a human neoplastic T-cell line probed with a fluorescent derivative of the envelope glycoprotein (gp120) of human immunodeficiency virus type 1 (HIV-1). *J. Cell. Physiol.*1991. **147**: 326–332.

25 Finnegan, C. M., Rawat, S. S., Cho, E. H., Guiffre, D. L., Lockett, S., MerrillJr., A. H. and Blumenthal, R., Sphingomyelinase restricts the lateral diffusion of CD4 and inhibits human immunodeficiency virus fusion. *J. Virol.* 2007. **81**: 5294–5304.

26 Rawat, S. S., Zimmerman, C., Johnson, B. T., Cho, E., Lockett, S. J., Blumenthal, R. and Puri, A., Restricted lateral mobility of plasma membrane CD4 impairs HIV-1 envelope glycoprotein mediated fusion. *Mol. Membr. Biol.* 2008. **25**: 83–94.

27 Xavier, R., Brennan, T., Li, Q., McCormack, C. and Seed, B., Membrane compartmentation is required for efficient T cell activation. *Immunity* 1998. **8**: 723–732.

28 Millan, J., Cerny, J., Horejsi, V. and Alonso, M. A., CD4 segregates into specific detergent-resistant T-cell membrane microdomains. *Tissue Antigens* 1999. **53**: 33–40.

29 Nguyen, D. H., Giri, B., Collins, G. and Taub, D. D., Dynamic reorganization of chemokine receptors, cholesterol, lipid rafts, and adhesion molecules to sites of CD4 engagement. *Exp. Cell. Res.* 2005. **304**: 559–569.

30 Maeda, F., Nagatsuka, Y., Ihara, S., Aotsuka, S., Ono, Y., Inoko, H. and Takekoshi, M., Bacterial expression of a human recombinant monoclonal antibody fab fragment against hepatitis B surface antigen. *J. Med. Virol.* 1999. **58**: 338–345.

31 Shimizu, S., Urano, E., Futahashi, Y., Miyauchi, K., Isogai, M., Matsuda, Z., Nohtomi, K. *et al.*, Inhibiting lentiviral replication by HEXIM1, a cellular negative regulator of the CDK9/cyclin T complex. *AIDS* 2007. **21**: 575–582.

32 Nagatsuka, Y., Hara-Yokoyama, M., Kasama, T., Takekoshi, M., Maeda, F., Ihara, S., Fujiwara, S. *et al.*, Carbohydrate-dependent signaling from the phosphatidylglucoside-based microdomain induces granulocytic differentiation of HL60 cells. *Proc. Natl. Acad. Sci. USA* 2003. **100**: 7454–7459.

Abbreviations: **B-LCL:** B-lymphoblastoid cell lines · **rhCD4:** recombinant human CD4 · **SHM:** somatic hypermutation

Full correspondence: Dr. Jun Komano, AIDS Research Center, National Institute of Infectious Diseases, 1-23-1 Shinjuku, Tokyo 162-864, Japan
Fax: +81-3-5285-1111
e-mail: ajkomano@nih.go.jp

Additional correspondence: Dr. Masataka Takekoshi, Department of Molecular Life Science, Division of Basic Molecular Science and Molecular Medicine, Tokai University School of Medicine, Isehara, Japan
e-mail: mtakekos@is.icc.u-tokai.ac.jp

Received: 2/4/2009
Revised: 22/12/2009
Accepted: 1/2/2010
Accepted article online: 16/2/2010

ANTIMICROBIAL AGENTS AND CHEMOTHERAPY, Sept. 2011, p. 4251–4260 Vol. 55, No. 9
0066-4804/11/$12.00 doi:10.1128/AAC.00299-11

Novel Postentry Inhibitor of Human Immunodeficiency Virus Type 1 Replication Screened by Yeast Membrane-Associated Two-Hybrid System▽

Emiko Urano,[1,2] Noriko Kuramochi,[3] Reiko Ichikawa,[2] Somay Yamagata Murayama,[1] Kosuke Miyauchi,[2] Hiroshi Tomoda,[3] Yutaka Takebe,[2] Milan Nermut,[4] Jun Komano,[2]* and Yuko Morikawa[1]*

Kitasato Institute for Life Sciences and Graduate School of Infection Control, Kitasato University, Shirokane 5-9-1, Minato-ku, Tokyo 108-8641, Japan[1]; AIDS Research Center, National Institute of Infectious Diseases, Toyama 1-23-1, Shinjuku-ku, Tokyo 162-8640, Japan[2]; Faculty of Pharmaceutical Sciences, Kitasato University, Shirokane 5-9-1, Minato-ku, Tokyo 108-8641, Japan[3]; and National Institute for Biological Standards and Control, South Mimms, Herts EN6 3QG, United Kingdom[4]

Received 3 March 2011/Returned for modification 25 April 2011/Accepted 1 July 2011

Human immunodeficiency virus (HIV) Gag protein targets to the plasma membrane and assembles into viral particles. In the next round of infection, the mature Gag capsids disassemble during viral entry. Thus, Gag plays a central role in the HIV life cycle. Using a yeast membrane-associated two-hybrid assay based on the SOS-RAS signaling system, we developed a system to measure the Gag-Gag interaction and isolated 6 candidates for Gag assembly inhibitors from a chemical library composed of 20,000 small molecules. When tested in the human MT-4 cell line and primary peripheral blood mononuclear cells, one of the candidates, 2-(benzothiazol-2-ylmethylthio)-4-methylpyrimidine (BMMP), displayed an inhibitory effect on HIV replication, although a considerably high dose was required. Unexpectedly, neither particle production nor maturation was inhibited by BMMP. Confocal microscopy confirmed that BMMP did not block Gag plasma membrane targeting. Single-round infection assays with envelope-pseudotyped and luciferase-expressing viruses revealed that BMMP inhibited HIV replication postentry but not simian immunodeficiency virus (SIV) or murine leukemia virus infection. Studies with HIV/SIV Gag chimeras indicated that the Gag capsid (CA) domain was responsible for the BMMP-mediated HIV postentry block. *In vitro* studies indicated that BMMP accelerated disassembly of HIV cores and, conversely, inhibited assembly of purified CA protein in a dose-dependent manner. Collectively, our data suggest that BMMP primarily targets the HIV CA domain and disrupts viral infection postentry, possibly through inducing premature disassembly of HIV cores. We suggest that BMMP is a potential lead compound to develop antiretroviral drugs bearing novel mechanisms of action.

Over 2 decades, research has developed antiretroviral therapy (ART) with a combination of antiretroviral drugs for human immunodeficiency virus type 1 (HIV-1) infection (10). ART has dramatically improved the survival of HIV-1-infected individuals. Current ART involves a combination of inhibitors of HIV-specific enzymes, such as protease (PR), reverse transcriptase (RT), and integrase (IN). In some cases, inhibitors of HIV-1 entry are also used. However, the emergence of HIV-1 variants resistant to antiretroviral drugs during ART stresses the need for novel HIV-1 inhibitors against distinct targets.

Multiple screening approaches have been employed for HIV-1 drug discovery (37) and have successfully discovered HIV-1 inhibitors that are currently available: nucleoside analogue RT inhibitors were discovered by HIV replication assays (23) and PR inhibitors were produced by structure-based drug design (25). In general, cell-free assays allow discovery of compounds with a relatively low 50% effective dose (ED_{50}) *in vitro*. However, many such compounds often fail to inhibit HIV-1 replication in *in vivo* assays, because they may not penetrate the cell membrane or may easily be catalyzed in metabolic environments. Also, possible toxic effects of the compounds must be tested in a subsequent cell culture study. In contrast, cell-based screens can exclude toxic compounds but have the disadvantages of time requirements and limitations on cell propagation in high-throughput screening.

Recently, cell-based assays using engineered cells and microorganisms have become an attractive alternative to *in vitro* assays for high-throughput screening. The yeast *Saccharomyces cerevisiae* is a convenient alternative to mammalian cells for this purpose. Comparative genomic analysis has shown that approximately 30% of yeast genes have homology to the mammalian protein sequences (8), indicating that basic cellular mechanisms are well conserved between yeast and human cells. Yeast has been used as a model organism for understanding biological functions of higher eukaryotic cells, leading to accumulation of scientific knowledge in yeast genetics and molecular biology. Such pioneering research has allowed the development of molecular technologies (e.g., two-hybrid assay and galactose induction), genetically modified cells (e.g., temperature sensitivity and conditional lethality), and cell selection systems (e.g.,

* Corresponding author. Mailing address for Jun Komano: AIDS Research Center, National Institute of Infectious Diseases, Toyama 1-23-1, Shinjuku-ku, Tokyo 162-8640, Japan. Phone: 81-3-5285-1111. Fax: 81-3-5282-5037. E-mail: ajkomano@nih.go.jp. Mailing address for Yuko Morikawa: Kitasato Institute for Life Sciences and Graduate School of Infection Control, Kitasato University, Shirokane 5-9-1, Minato-ku, Tokyo 108-8641, Japan. Phone: 81-3-3444-6161. Fax: 81-3-5791-6268. E-mail: morikawa@lisci.kitasato-u.ac.jp.

▽ Published ahead of print on 11 July 2011.

URA3 nutritional selection), enabling the construction of simple readout assay systems.

Gag protein, the main structural component of retrovirus, directs particle assembly. HIV Gag protein is synthesized as a precursor protein, p55, which is composed of matrix (MA), capsid (CA), nucleocapsid (NC), and p6 domains, and cotranslationally myristoylated at the N-terminal glycine. Concomitant with the N-terminal myristoylation, p55Gag is targeted to the plasma membrane and assembled into virus particles (13, 22). During particle release, Gag undergoes proteolytic processing to generate the CA domain that forms the mature capsid. In the next round of infection, the mature capsid disassembles during viral penetration into host cell cytoplasm. Thus, the capsid assembly and disassembly are reverse reactions during virus release and entry and must be regulated by yet-unknown mechanisms. Indeed, the optimal stability of HIV-1 capsid is required for efficient infection (14). We have previously shown that the particle assembly process is reproducible in a yeast cell system (26). Here, we further developed a yeast membrane-associated two-hybrid assay system in which a temperature-sensitive mutant strain of yeast grows at restrictive temperature when Gag-Gag interactions occur. Using this yeast two-hybrid system, we have screened a chemical library composed of 20,000 low-molecular-weight compounds and have found a compound that targets CA-CA interactions and inhibits HIV-1 replication.

MATERIALS AND METHODS

Construction and transformation of yeast expression plasmids. A yeast membrane-associated two-hybrid assay based on the CytoTrap SOS recruitment system (Stratagene) was employed in this study. The full-length *gag* gene of HIV-1 (HXB2 strain) was placed downstream of the yeast inducible promoter for the *GAL1* gene in frame with the cDNA of SOS in a pSOS plasmid (Stratagene) that contains the *LEU2* gene as a yeast selective marker. The HIV-1 (HXB2 strain) *gag* gene was also cloned into pMyr plasmid, which contains a yeast inducible promoter for the *GAL1* gene and the *URA3* gene as a selective marker. The *S. cerevisiae* strain cdc25Ha (*MAT***a** *ura3-52 his3-200 ade2-101 lys2-801 trp1-901 leu2-3 112 cdc25-2* Gal^+) was doubly transformed with the yeast expression plasmids.

Chemical library screening in CytoTrap yeast membrane-associated two-hybrid system. Yeast transformants were initially grown at 25°C in synthetic defined medium with glucose (0.67% yeast nitrogen base, 2% glucose, and amino acid mixtures without uracil or leucine) (permissive conditions). After being washed, culture was diluted to an optical density at 600 nm (OD_{600}) of 0.1 in synthetic defined medium with galactose and raffinose (0.67% yeast nitrogen base, 2% galactose, 2% raffinose, and amino acid mixtures without uracil or leucine) for Gag expression. The yeast culture (OD_{600} = 0.1) was incubated with a chemical library (a final concentration of 10 μM) at 37°C for 5 days (restrictive conditions) in 96-well microtiter plates with shaking. The chemical library (preplated Diversity Set) was purchased from Enamine. After complete resuspension of cells by vortexing of microtiter plates, cell density was measured at 600 nm by a plate reader (Infinite200; Tecan).

Mammalian cells and transfection. 293T, HeLa, and MT-4 cells were provided by the AIDS Research Center, National Institute of Infectious Diseases, Japan. 293FT cells were purchased from Invitrogen. Peripheral blood monocytic cells (PBMC) were isolated by Ficoll-Conray density centrifugation from healthy donors. All mammalian cells were maintained in RPMI 1640 medium (Sigma) supplemented with 10% fetal bovine serum (Japan Bioserum, Japan), 100 U/ml penicillin, and 100 mg/ml streptomycin (Invitrogen), at 37°C in a humidified 5% CO_2 atmosphere. For PBMC culture, GlutaMax-I (Invitrogen), insulin-transferrin-selenium A (Invitrogen), 200 ng/ml anti-CD3 monoclonal antibody (OKT3; Janssen Pharmaceutical), and 70 U/ml recombinant human interleukin-2 (IL-2; Shionogi Pharmaceutical, Japan) were further added to the medium. Transfection was carried out with Lipofectamine 2000 according to the manufacturer's protocol (Invitrogen).

Cell toxicity assays. For determining the toxicity of the chemical library to yeast, yeast cultures were diluted to an OD_{600} of 0.01 and incubated under permissive conditions (at 25°C in glucose medium) with the chemical library. After 2 days, cell density was measured at 600 nm by a plate reader (Infinite200; Tecan). For determining toxicity to mammalian cells, 293T, 293FT, HeLa, and MT-4 cells and PBMC were incubated with compounds at 37°C for 2 to 14 days and subjected to 3-(4,5-dimethylthiazol-2-yl)-5-(3-carboxymethoxyphenyl)-2-(4-sulfophenyl)-2H-tetrazolium (MTS) and Alamar Blue assays according to the manufacturer's instructions. The OD of the MTS assay mixture was measured at 490 nm, and the OD of the Alamar Blue assay mixture was measured at 570 nm by a plate reader (FLx800; BioTek). The 50% cytotoxicity concentrations were defined as drug concentrations by which the OD values reached the 50% level of the no-drug (dimethyl sulfoxide [DMSO]) controls.

HIV-1 replication assays. MT-4 Luc cells that were transduced with luciferase in MT-4 cells (31) and PBMC were grown in RPMI 1640 medium supplemented with 10% fetal bovine serum. MT-4 Luc cells were infected with HIV-1 (HXB2 strain) corresponding to 1.25 ng of p24CA antigen and incubated at 37°C in the presence of compounds. On day 7, MT-4 Luc cells were subjected to luciferase assay. PBMC were stimulated with IL-2 and anti-CD3 antibody. Following infection with HIV-1 (HXB2 strain) corresponding to approximately 5 ng of p24CA antigen, PBMC were incubated at 37°C and passaged every 3 to 4 days in the presence of compounds. The culture supernatants of PBMC were temporally collected and subjected to quantification of HIV-1 particle yields by p24CA antigen capture enzyme-linked immunosorbent assay (ELISA; Zeptometrix).

Single-round infection assays. For single-round infection assays, HIV-1 was pseudotyped with either HIV-1 Env protein or vesicular stomatitis virus (VSV) G protein as described previously (35). Briefly, 293FT cells were transfected with a plasmid containing the codon-optimized HXB2 *gag-pol* gene (pHIVgag-pol), a lentiviral plasmid expressing luciferase (pLenti-luciferase), a plasmid expressing HIV-1 Rev (pRevpac), and either a plasmid expressing HIV-1 Env or a plasmid expressing VSV-G. Culture media were harvested and inoculated into MT-4 and 293FT cells in the presence of 5 to 10 μg/ml dextran (ICN). HIV-1 pseudotyped with autologous HIV-1 Env protein was inoculated into 293FT-CD4 (expressing CD4 constitutively) cells. On day 2 or 3, infectivity was assessed by luciferase activity transduced by pLenti-luciferase. HIV-1 (NL43 strain) expressing luciferase, simian immunodeficiency virus (SIV) (mac239 strain), and murine leukemia virus (MLV) (Moloney strain) were similarly pseudotyped with VSV-G (28). The viruses were enriched by centrifugation through sucrose cushions if necessary.

HIV/SIV Gag chimeras were generated in the context of pHIVgag-pol by replacing the MA and CA domains with the SIV MA and CA domains, respectively. The Gag chimeras contain the cleavage site sequences of HIV-1 Gag at the chimera junctions. Amino acid substitutions G89A and P90A in the cyclophilin A (CypA)-binding loop of CA (corresponding to Gag amino acid positions 225 and 226) (11, 16) were carried out by overlap PCR in the context of pHIVgag-pol.

Quantitative PCR for HIV-1 cDNA synthesis. MT-4 cells were infected with HIV-1 (HXB2 strain) and incubated in the presence of compounds. Efavirenz (EFV) was provided by the NIH AIDS Research and Reference Reagent Program and was used as positive control. The cellular genomic DNA was extracted 4 and 24 h postinfection with a DNeasy kit (Qiagen) according to the manufacturer's instructions. The cellular DNA was subjected to quantitative real-time PCR using the Quantitec probe PCR kit containing SYBR green (Qiagen). The following primer sets were used: 5′-AACTAGGGAACCCACTGCTTAAG-3′ and 5′-CTGCTAGAGATTTTCCACACTGAC-3′ (specific for the R-U5 region in early reverse transcripts of HIV-1 cDNA), 5′-CCGTCTGTTGTGTGACTC TGGT-3′ and 5′-GAGTCCTGCGTCGAGAGAGCT-3′ (specific for the late reverse transcripts of HIV-1 cDNA), 5′-TGCTGGGATTACAGGCGTGAG-3′ and 5′-CTGCTAGAGATTTTCCACACTGAC-3′ (specific for long terminal repeat [LTR] and *Alu* region in the integrated HIV-1 cDNA), and 5′-AACTAG GGAACCCACTGCTTAAG-3′ and 5′-CTGCTAGAGATTTTCCACACTGA C-3′ (second PCR) (specific for LTR region in the integrated HIV-1 cDNA) (12). The amplification kinetics was monitored by the Opticon 2 system (Bio-Rad). The levels of cellular DNA were normalized by the levels of β-globin DNA quantified using primers 5′-TATTGGTCTCCTTAAACCTGTCTTG-3′ and 5′-CTGACACAACTGTGTTCACTAGC-3′ (19).

Viral protein expression and particle purification. HIV-1 proviral clone pHXB2 was transfected into 293FT and HeLa cells in the presence of increasing doses of 2-(benzothiazol-2-ylmethylthio)-4-methylpyrimidine (BMMP). After 2 days, cells were analyzed by Western blotting using anti-HIV-1 p24CA monoclonal antibody (100-fold diluent of 183-H12-5C hybridoma culture supernatant; NIH AIDS Research and Reference Reagent Program). HIV particles were collected by centrifugation through 20% (wt/vol) sucrose cushions in an SW55

rotor (Beckman Coulter) at 120,000 × *g* for 1 h. For HIV/SIV Gag chimeras, 293FT cells were cotransfected with pHIVgag-pol expressing Gag chimera, pLenti-luciferase, pRevpac, and a plasmid expressing VSV-G. Cells and purified particles were similarly analyzed by Western blotting using anti-HIV-1 p24CA, anti-HIV-1 p17MA (2 μg/ml; 13-103-100; Advanced Biotechologies), and anti-SIV p27CA (1 μg/ml; 4324; Advanced Bioscience Laboratories) monoclonal antibodies.

***In vitro* assembly reaction of CA.** The *in vitro* assembly reaction of CA was performed as described previously (17, 36). Briefly, the purified HIV-1 CA (a final concentration of 100 μM) was incubated at 37°C for 1 h in buffer containing 20 mM Tris (pH 8.0), 500 mM NaCl, 0.2 mM EDTA, and 1 mM dithiothreitol. Assembly products were pelleted by centrifugation at 18,000 × *g* for 30 min at 4°C and were subjected to p24CA antigen capture ELISA (Zeptometrix) and electron microscopy.

***In vitro* disassembly reaction of capsid cores.** The *in vitro* disassembly assay was performed according to Aiken's method with some modifications (3). HIV particles were purified by ultracentrifugation through 20% (wt/vol) sucrose cushions. For isolation of HIV capsid cores, purified HIV particles were applied onto sucrose step gradients composed of 7.5% (wt/vol), 15% (wt/vol) containing 1% Triton X-100, and 30 to 70% (wt/vol) sucrose and subjected to centrifugation at 120,000 × *g* for 16 h at 4°C. Fractions rich in HIV cores were collected and resuspended in buffer (10 mM Tris [pH 7.4], 100 mM NaCl, and 1 mM EDTA). For core disassembly assays, aliquots of HIV cores were incubated at 37°C in the presence of compounds. For comparison, azidothymidine (AZT) (Moravek Biochemicals) was added to the reaction mixture. Intact cores were recovered by centrifugation at 125,000 × *g* for 30 min at 4°C.

Confocal microscopy and electron microscopy. HeLa cells were transfected with a pNL43 derivative expressing Gag-green fluorescent protein (GFP) fusion protein but not *pol* gene products. Cells were fixed with 3.7% paraformaldehyde in phosphate-buffered saline (PBS) for 30 min at room temperature and were treated with 0.1% Triton X-100 for 10 min at room temperature for membrane permeabilization. Following nuclear staining with TO-PRO-3 (Molecular Probes), cells were mounted with antibleaching reagent and observed with a laser scanning microscope (TCS; Leica).

In vitro assembly products were adsorbed onto carbon-coated copper grids and stained with 2% (wt/vol) uranyl acetate. Sections were subjected to electron microscopy.

Statistical analysis. Intergroup comparisons were performed with paired *t* test (for parametric group analysis). All *P* values were considered significant if less than 0.05.

RESULTS

A yeast membrane-associated two-hybrid system for HIV-1 Gag-Gag interactions. For construction of a yeast cell-based Gag assembly system, we employed a yeast membrane-associated two-hybrid assay based on the CytoTrap SOS recruitment system (Stratagene) in this study (Fig. 1). For HIV-1 Gag expression, two yeast expression plasmids, pMyr and pSOS, were used: pMyr contains the yeast inducible promoter for the *GAL1* gene followed by a myristoylation signal (amino acid sequence, MGSSKSKPKDPSQRR) for membrane targeting and pSOS contains the constitutive promoter for the yeast *ADH* gene followed by the human SOS gene. The *gag* gene of HIV-1 (HXB2 strain) was cloned in frame with the myristoylation signal in pMyr. The *gag* gene was similarly cloned in frame with the SOS gene in pSOS that allowed production of SOS-Gag fusion protein (Fig. 1A). The *S. cerevisiae* cdc25H strain was doubly transformed with these Gag expression plasmids. The cdc25H strain contains a temperature-sensitive mutation in the CDC25 gene, which allows growth at 25°C (permissive temperature) but not at 37°C (restrictive temperature). SOS is the human orthologue of the yeast CDC25 and can activate the yeast RAS signal transduction pathway that complements the yeast *cdc25* defect (4). When myristoylated Gag and SOS-Gag are coexpressed in the cdc25H cells, the SOS-Gag is recruited to the plasma membrane through an interaction with the myristoylated Gag, leading to growth of the cdc25H cells at 37°C (Fig. 1B). We initially confirmed that the cdc25H cells transformed with the Gag/pMyr and Gag/pSOS plasmids grew at 37°C in galactose plus raffinose medium under conditions in which SOS-Gag fusion protein was expressed but not at 37°C in glucose medium under conditions in which SOS-Gag fusion was not expressed.

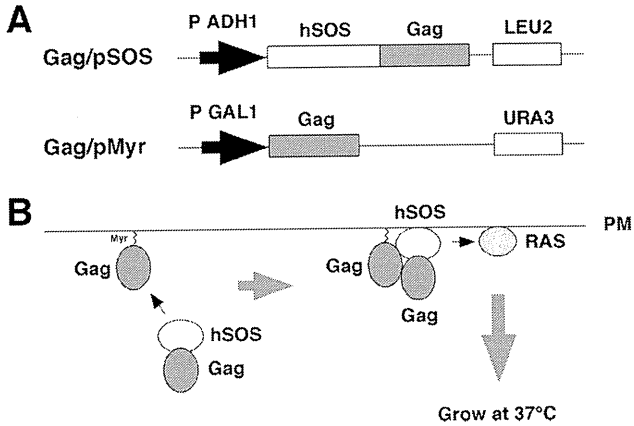

FIG. 1. Yeast membrane-associated two-hybrid screening for inhibitors of Gag-Gag interaction. (A) Schematic representation of Gag expression plasmids used for yeast SOS recruitment system. The full-length *gag* gene of HIV-1 (HXB2 strain) was expressed by yeast expression plasmids pMyr and pSOS: pMyr contains the yeast inducible promoter for the *GAL1* gene and the *URA3* gene as a selective marker and pSOS contains the constitutive promoter for the yeast *ADH* gene and the *LEU2* gene as a selective marker. (B) Principle of yeast membrane-associated two-hybrid assay based on SOS recruitment system. The schematic illustration was adapted with permission from the manuals for the CytoTrap yeast system (Agilent Technologies, Inc.; http://www.genomics.agilent.com/CollectionSubpage.aspx?PageType=Product&SubPageType=ProductDetail&PageID=1311).

Screening of a chemical library for Gag-Gag interaction inhibitors by yeast membrane-associated two-hybrid assays. For screening for inhibitors of Gag assembly, we optimized this yeast membrane-associated Gag-Gag interaction system to a liquid format using 96-well microplates. Using this system, we screened a chemical library composed of 20,000 compounds, each of which was initially designated by the numbers of microplates and wells of the chemical library (e.g., 172A6 indicates microplate number 172 and well number A6). When the cdc25H transformant was incubated at 37°C in galactose plus raffinose medium with a chemical library (10 μM each), we found 10 compounds that reduced cell growth (Fig. 2A, black columns). To examine if cell growth reduction is specifically due to the disruption of Gag-Gag interaction, we used another cdc25H transformant that contained MAFB/pSOS and SOS binding protein/pMyr plasmids. This combination produces SOS-MAFB fusion protein and myristoylated SOS binding protein and can be used as a positive control for the CytoTrap system (Stratagene). When using this positive control, we observed that 4 compounds (2G5, 73A7, 189A9, and 235C2) out of the 10 compounds also reduced cell growth (Fig. 2A, white columns), suggesting that they might inhibit pathways which are commonly used in the CytoTrap system (e.g., N myristoylation and RAS signaling). Thus, we concluded that 6 compounds (1G5, 31E7, 34A8, 73A5, 147B2, and 172A6) specifi-

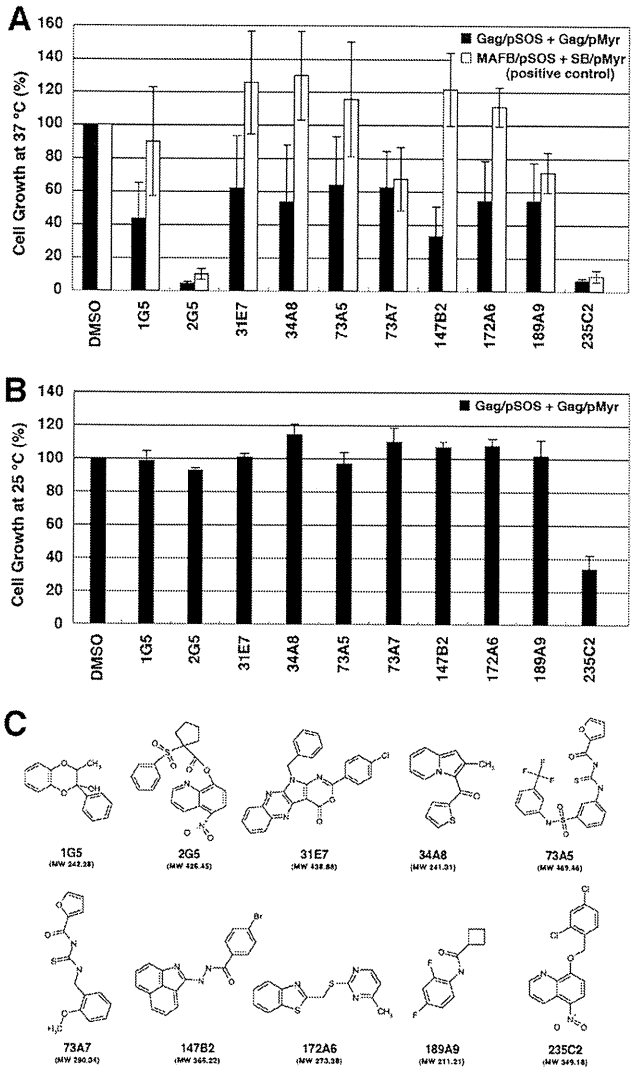

FIG. 2. Screening for inhibitors of Gag assembly by yeast membrane-associated two-hybrid assays. (A) The yeast cdc25Ha strain was transformed with the pSOS and pMyr plasmids. The yeast culture was diluted to an OD_{600} of 0.1 and incubated at 37°C in galactose-plus-raffinose medium (restrictive conditions) with a chemical library (a final concentration of 10 μM). After growth at 37°C for 5 days, cell density was measured at OD_{600}. As a control, the OD_{600} of yeast incubated in the presence of DMSO was set to 100%. The yeast transformed with the pSOS and pMyr plasmids, both of which contained the HIV-1 *gag* gene, was shown as black columns, and the yeast was transformed with the pSOS plasmid containing MAFB and the pMyr plasmid containing the cDNA of SB (as a positive-control combination) as white columns. Data were shown as means with standard deviations from 5 independent experiments. (B) The yeast cdc25Ha strain transformed with the pSOS and pMyr plasmids containing the HIV-1 *gag* gene was grown at 25°C in glucose medium. The yeast culture was diluted to an OD_{600} of 0.01 and incubated at 25°C in glucose medium with a chemical library (a final concentration of 10 μM). After growth at 25°C for 2 days, cell density was measured at OD_{600}. As a control, the OD_{600} of yeast incubated in the presence of DMSO was set to 100%. Data were shown as means with standard deviations from 3 independent experiments. (C) Structures of compounds screened from a chemical library by yeast membrane-associated two-hybrid assays.

cally inhibited a Gag-Gag interaction. No common chemical structures were found among the 6 candidates. However, 3 chemicals (34A8, 147B2, and 172A6) share relatively similar structures whereby two allyl groups are connected by a short linker moiety. To test the cell toxicity, the cdc25H transformants were incubated at 25°C in glucose medium (permissive conditions) with the compounds (10 μM each) (Fig. 2B). All the compounds except 235C2 allowed cell growth at levels comparable to that obtained in the presence of DMSO (as a control). Further studies revealed that 235C2 preferentially inhibited growth of several fungi *in vitro* (e.g., *Candida albicans* and *Aspergillus fumigatus* at MICs of 5.7 and 10 μM, respectively) (data not shown), suggesting that it might serve as a lead compound to develop an antifungal agent. The chemical formulas of 10 compounds are shown in Fig. 2C.

Inhibition of HIV replication in mammalian cells by compounds identified as yeast membrane-associated Gag-Gag interaction inhibitors. We evaluated the anti-HIV activity of the 6 candidates in mammalian cell systems. MT-4 Luc cells (human T lymphocytic cell line expressing luciferase constitutively) were infected with HIV-1 (HXB2 strain) and incubated at 37°C in the presence of the test compounds. In this T cell system, the luciferase activity is reduced by HIV-1 infection, due to the cell death upon HIV-1 replication (31). When added to HIV-1-infected MT-4 Luc cells, one of the candidates (172A6) recovered the luciferase expression in a dose-dependent manner (Fig. 3A), indicating that 172A6 was capable of reduction in HIV replication in mammalian cells. When 293T cells were incubated with the 6 compounds and were subjected to Alamar Blue assays, none of the compounds showed apparent reduction in cell viability (Fig. 3B). To confirm the anti-HIV effect, PBMC were infected with HIV-1 in the presence of 172A6 and production of HIV in the culture medium was temporally measured by p24CA antigen capture ELISA. 172A6 limited HIV replication at 5 μM and severely inhibited it at 25 μM (Fig. 3C, upper panel). When uninfected PBMC were similarly exposed to 172A6 and assessed by MTS assays, a slight reduction in cell viability was observed at 25 μM (Fig. 3C, lower panel). However, the severe inhibition of HIV replication at 25 μM 172A6 could not be ascribed fully to its cytotoxic effect. Using several mammalian cell lines, we reevaluated cytotoxicity of 172A6 by MTS assays. No significant cytotoxicity of 172A6 was seen in the cell lines, except in PBMC, that we used in this study (Fig. 3D). Based on the chemical structure [2-(benzothiazol-2-ylmethylthio)-4-methylpyrimidine] of the compound 172A6 (Fig. 2C), we called it BMMP here.

No inhibition of HIV particle release by BMMP. We initially examined whether BMMP inhibited HIV-1 particle production. 293FT cells were transfected with pHXB2 and incubated at 37°C in the presence of 5 to 50 μM BMMP. Western blotting using anti-HIV-1 p24CA antibody revealed that the intracellular level of Gag expression and the pattern of Gag processing were largely unaffected in the presence of BMMP (Fig. 4A), suggesting that BMMP did not inhibit HIV protease. When purified particle fractions were similarly analyzed, we found no reduction in particle production (Fig. 4A). We obtained similar results on HeLa cells. This indicates that BMMP did not block HIV-1 particle release.

Intracellular distribution of Gag was examined by confocal

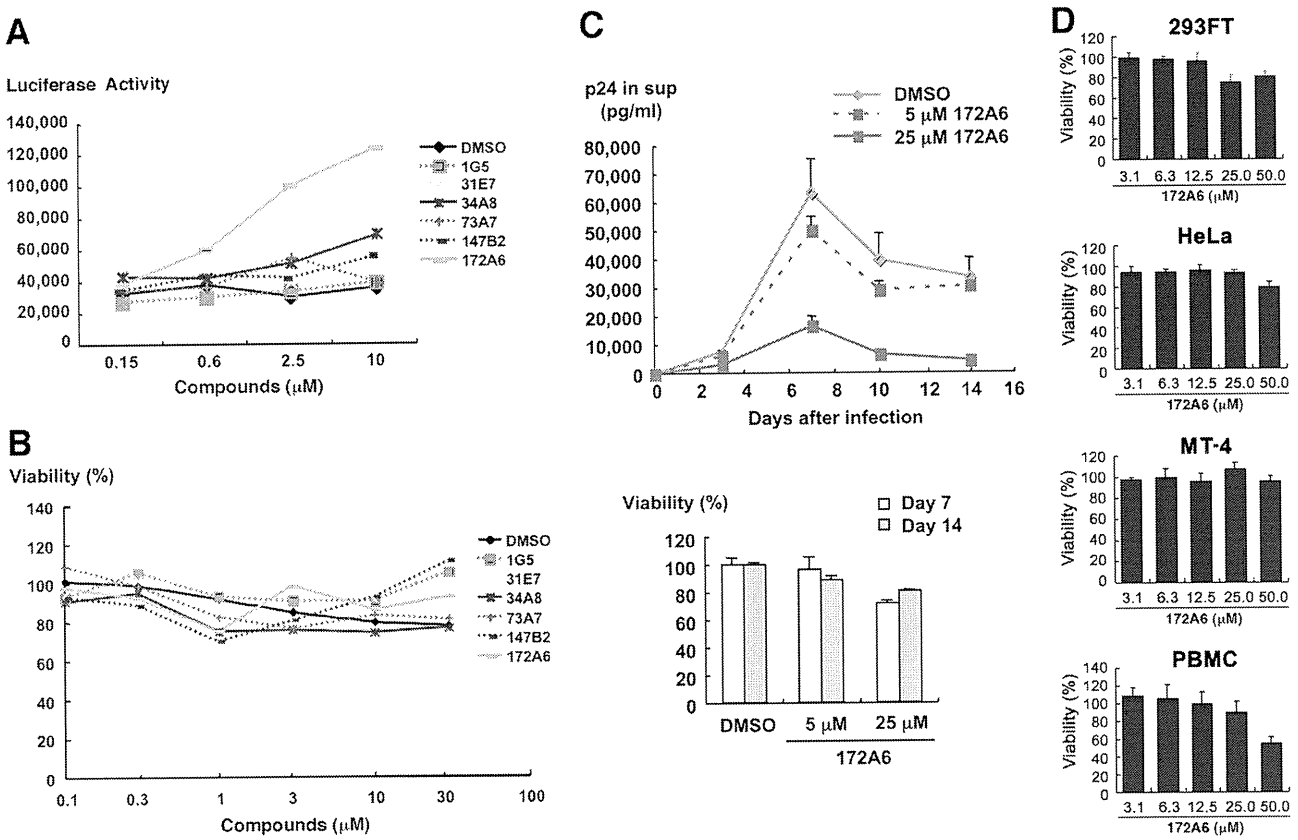

FIG. 3. Inhibition of HIV-1 replication and cell toxicity. (A) MT-4 Luc cells were infected with HIV-1 (HXB2 strain) and incubated at 37°C in the presence of increasing doses of compounds. On day 7, MT-4 Luc cells were subjected to luciferase assay. Data were shown as means from triplicate cultures. (B) 293T cells were incubated with various doses of compounds at 37°C for 2 days and subjected to Alamar Blue assays. Data were shown as means from 3 independent experiments. (C) PBMC stimulated with IL-2 and anti-CD3 antibody were infected with HIV-1 (HXB2 strain) and incubated at 37°C in the presence of 5 and 25 μM 172A6. HIV-1 production in culture medium was temporally quantified by p24CA antigen capture ELISA (top). Uninfected PBMC were cultured with 172A6 at 37°C and were subjected to MTS assay on days 7 and 14. Data were shown as means with standard deviations from triplicate cultures, in which DMSO was used as control. (D) 293FT, HeLa, and MT-4 cells and PBMC were incubated at 37°C with various doses of 172A6 and were subjected to MTS assay on days 4, 3, 4, and 6, respectively. Cell viability was shown as OD_{490}. Data were shown as means with standard deviations from triplicate cultures.

microscopy (Fig. 4B). HeLa cells were transfected with a pNL43 derivative that expresses Gag-GFP and incubated with 30 μM BMMP. Gag-GFP was distributed predominantly at the plasma membrane in cells treated with DMSO (used as control). A similar Gag-GFP distribution was observed in cells treated with BMMP, indicating that BMMP did not inhibit Gag targeting to the plasma membrane, consistent with the above findings.

Inhibition of HIV replication postentry by BMMP. To examine whether BMMP exerted an inhibitory effect on early stages of the HIV life cycle, such as viral entry, we employed single-round infection assays with luciferase-expressing HIV-1 vectors which were pseudotyped with either VSV-G or authentic HIV-1 Env protein. To this end, pHIVgag-pol (for expression of HIV-1 Gag and Gag-Pol), pRevpac (for expression of HIV-1 Rev), and pLenti-luciferase vector, which provides the artificial lentiviral genome expressing luciferase driven by cytomegalovirus promoter, were cotransfected with either VSV-G or authentic HIV-1 Env expression plasmid into 293FT cells. HIV-1 Luc viruses produced were inoculated into MT-4 cells in the presence of BMMP, and viral infectivity was monitored by a luciferase reporter assay. Luciferase expression was inhibited in a BMMP dose-dependent manner in cells infected with the HIV-1 Env-pseudotyped Luc virus, indicating that BMMP inhibited the early stage of the HIV-1 life cycle (Fig. 5A). However, when VSV-G-pseudotyped Luc virus was used, a dose-dependent reduction was similarly observed. When HIV-1 (NL43 strain) expressing luciferase was pseudotyped with VSV-G and used in this assay, the luciferase activity driven by the LTR promoter was similarly reduced in the presence of BMMP, suggesting that BMMP did not inhibit the stage of HIV entry (e.g., attachment and membrane fusion processes) but the stage of postentry (e.g., uncoating) (Fig. 5A). The Env-independent infectivity reduction was confirmed when HIV-1 Luc viruses were inoculated into 293FT and 293FT-CD4 cells (Fig. 5B). We examined whether BMMP also blocked the postentry stage of SIV. Interestingly, single-round infection assays with luciferase-expressing SIVmac239 vectors which were pseudotyped with VSV-G protein showed no inhibition of luciferase expres-